PARTE 1

TEMAS DE INTERESSE DA CONVENÇÃO ANUAL DO AIUM DE 2012 – DE 29 DE MARÇO A 1 DE ABRIL, REALIZADO EM PHOENIX, ARIZONA – EUA

Relato de Lucy Kerr da sua participação na convenção e pré-convenção

A convenção iniciou-se em 30 de março de 2012 com sessões **APENAS DE IMAGEM E DE REVISÃO COMPREENSIVA DE ASSUNTOS IMPORTANTES** e sempre são abordados vários temas concomitantemente em salas distintas. Havia para se escolher entre escroto agudo e dor pélvica, cardiologia fetal desconhecida, imagem ultrassonográfica dinâmica de músculo esquelético, ultrassom de malformações perinatais e do abdômen perinatal, esticando protocolo, técnica de revisão vascular com vários casos exemplificados, status atual da liberação do contraste ultrassonográfico pelo FDA nos EUA, prognóstico e aconselhamento em anomalias fetais, apresentando casos de sobreviventes após diagnóstico US e atualização na neurossonografia fetal e neonatal. Escolhemos a aula **DE PELVA AGUDA,** moderada por Leslie Scoutt, que vamos sumarizar os principais aspectos:

A primeira apresentação foi de Harris L. Cohen que relatou uma peculiaridade do paciente pediátrico **com, ESCROTO AGUDO**, pode apresentar testículos de tamanhos muito variáveis, o que é normal, mas o escroto realmente pequeno exige avaliação. Nos primeiros meses de vida os testículos mostram ecogenicidade bem homogênea E recomenda que o examinador tenha muita paciência na avaliação escrotal da criança que pode revelar-se muito valiosa. Quando o paciente dá entrada com dor testicular aguda as principais perguntas que o ultrassonografista deve formular são:

- Há fratura testicular?
- Há hematoma testicular?
- Há torção aguda?
- Não é possível detectar a causa?

A seguir foram mostrados vários casos, com imagens bem elucidativas.

1º caso: uma criança de 6 anos com dor escrotal, testículos pequenos mas Doppler normal. Pergunta: é normal? A análise mais detalhada das imagens mostra uma massa acima do testículo e acolada a ele compatível com torção do apêndice testicular ou do apêndice do epidídimo. Durante a discussão, o professor relata que existem pelo menos cinco apêndices na bolsa escrotal, os quais são remanescentes embriológicos, mas três deles são os mais comuns:

- Apêndice do epidídimo;
- Apêndice do testículo;
- Vasa aberrantes.

A torção do apêndice testicular ocorre mais comumente dos 6 aos 12 anos, provocando dor, edema e eritema local e ele é responsável por 35% das causas do escroto agudo. Usualmente o apêndice testicular normal só é detectado quando há pequena hidrocele associada, mas é bem mais fácil identificá-lo quando está aumentado.

2º caso: um adolescente de 15 anos com dor escrotal intensa há quarto dias. A US mostrou testículo direito aumentado, difusamente hipoecogênico e com focos de hiperecogenicidade

esparsos. As hipóteses diagnósticas principais seriam hemorragia testicular ou torção, pois tanto as áreas necróticas são hipoecóicas, quanto as áreas de hemorragia, embora estas últimas exibam com freqüência áreas de hiperecogenicidade. A chave para o diagnóstico diferencial é o Doppler colorido: se houver fluxo no tecido testicular remanescente, muitas vezes permeando o hematoma, trata-se de hemorragia, mas se houver ausência total de fluxo trata-se de torção antiga, que era o caso.

3º caso: um paciente com dor testicular esquerda de instalação recente. A US revelou textura testicular normal bilateralmente. O estudo Doppler demonstrou testículo direito com fluxo normal, tanto no mapa a cores como no Doppler pulsátil, enquanto que no testículo havia ausência de fluxo. Conclusão: é torção testicular. Para fazer o diagnóstico de torção testicular é necessário olhar para o padrão textural e de vascularização, embora a chave diagnóstica seja a ausência de fluxo. A causa mais comum de testículo agudo é a torção e os sintomas dependem da duração da torção, do número de torções e de quão apertada é a torção dos vasos. A injúria da espermatogênese ocorre em apenas seis horas. Os sintomas da torção se sobrepõem aos da epididimite, orquiepididimite, torção do apêndice testicular ou do epidídimo e hérnia estrangulada. O autor citou uma publicação onde os autores fazem uma revisão e relato de sinal específico da torção testicular:

Sonographic Differential Diagnosis of Acute Scrotum

Real-time Whirlpool Sign, a Key Sign of Torsion

1. **S. Boopathy Vijayaraghavan, MD, DMRD**

+ Author Affiliations/; *Sonoscan Ultrasonic Scan Centre, Coimbatore, India.*

Abstract

Objective. The purpose of this study was to prospectively investigate the role of high-resolution and color Doppler sonography in the differential diagnosis of acute **scrotum** and testicular torsion in particular. ***Methods.*** Patients who underwent sonography for acute **scrotum** between April 2000 and September 2005 were included in the study. Gray scale and color Doppler sonography of the **scrotum** was performed. The spermatic cord was studied on longitudinal and transverse scans from the inguinal region up to the testis, and the whirlpool sign was looked for. ***Results.*** During this period, 221 patients underwent sonography for acute **scrotum**. Sixty-five had epididymo-orchitis with a straight spermatic cord, a swollen epididymis, testis, or both, an absent focal lesion in the testis, and increased flow on color Doppler studies along with the clinical features of infection. Three had testicular abscesses. Sonography revealed features of torsion of testicular appendages in 23 patients and acute idiopathic scrotal edema in 19. Complete torsion was seen in 61 patients who had the whirlpool sign on gray scale imaging and absent flow distal to the whirlpool. There was incomplete torsion in 4 patients in whom the whirlpool sign was seen on both gray scale and color Doppler imaging. Nine patients had segmental testicular infarction, and 1 had a torsion-detorsion sequence revealing testicular hyperemia. In 14 patients, the findings were equivocal. There was a complicated hydrocele, mumps orchitis, and vasculitis of Henoch-Schönlein purpura in 1 patient each. Five patients had normal findings. Fourteen were lost for follow-up. ***Conclusions.*** Sonography of acute **scrotum** should include study of the spermatic cord. The sonographic real-time whirlpool sign is the most specific and sensitive sign of torsion, both complete and incomplete. Intermittent testicular torsion is a challenging clinical condition with a spectrum of clinical and sonographic features. **acute scrotum,color Doppler sonography, segmental infarction, sonography, testicular torsion, whirlpool sign, ITT, intermittent testicular torsion**

Acute scrotal pain may have many causes. The more common causes are testicular torsion, epididymo-orchitis, torsion of the testicular appendages, and acute idiopathic scrotal edema. The most important aim of imaging in these patients is to rule in or out testicular torsion, which warrants emergency surgery to avoid testicular impairment. At the same time, the investigation should be specific enough to avoid unnecessary surgery. Testicular torsion can be extravaginal, intravaginal, or mesorchial. Intravaginal torsion, the most common type, occurs between 3 and 20 years of age, with an incidence of 65% between 12 and 18 years.[1] It is generally associated with a preexisting anomaly of fixation of the testis, termed “bell and clapper testis.” Here the

intrascrotal portion of the spermatic cord lacks posterior adhesion to the **scrotum** and remains surrounded by the tunica vaginalis, thus predisposing to rotation of the testis and cord. A 12% incidence of bell clapper deformity was found in one autopsy series.[2] The horizontal lie of the testis has been linked with the bell clapper deformity in 100% of patients who have had surgery.[3-5] In most people, this anomaly is bilateral,[5] which warrants orchidopexy of the contralateral testis in cases of torsion of the testis. This procedure is necessary to avoid the risk of metachronous torsion of the contralateral testis and anorchia, the reported incidence of which is 30% to 43% of cases.[6-8] Hence, a definitive diagnosis of testicular torsion is essential even in cases with late appearance, partial torsion, or intermittent testicular torsion (ITT). Even though there are clinical signs of differentiation between the various conditions causing acute **scrotum**, they are not accurate. There are gray scale sonographic features of the testis and its environment in differentiating these conditions, but they fail in accuracy. High-resolution color Doppler sonography has been shown to be the most accurate and important modality in the differential diagnosis of acute scrotal pain,[9-12] but there are some difficulties encountered. Arce et al[13] and Baud et al[14] described rotation of the cord as a very useful sign of acute spermatic cord torsion. More recently, the incidence of ITT or the torsion-detorsion sequence with a varying spectrum of clinical and sonographic features has been reported by many authors.[3,4,15-18] Intermittent testicular torsion is a clinical syndrome defined by a history of unilateral scrotal pain of sudden onset and of short duration that resolves spontaneously.[15] The intensity of pain may or may not be as severe as that seen with acute torsion. The mean number of painful episodes reported is 4.3, and the range is 1 to 30 over 2 to 48 months.[3,5,16] The mean age of initial appearance is reportedly 12 years (range, 1.7 to 58 years).[3,5,17] The objective of this study was to prospectively investigate the role of high-resolution and color Doppler sonography in the differential diagnosis of acute **scrotum** and testicular torsion in particular, with a real-time technical modification of the sign of rotation of the cord in the form of the whirlpool sign.

Materials and Methods

All patients who had acute pain with or without swelling of the **scrotum** between April 2000 and September 2005 were included in the study. The ages of the patients and the clinical features were recorded. There were no laboratory investigations available at the time of sonography. High-resolution sonography and color Doppler sonography were done on all the patients with a Linear 5- to 12-MHz probe (HDI 3500 and HDI 5000; Philips Medical Systems, Bothell, WA). Gray scale imaging started in the inguinal region of the symptomatic side and extended along the spermatic cord to end in the **scrotum**. Both longitudinal and transverse scans were done. The following features were looked for: (1) tortuosity of the cord, (2) an acute change in the direction of the cord, and (3) the presence of the whirlpool sign. The whirlpool sign was elicited in the following manner. When tortuosity of the spermatic cord was seen, a short axis scan of the cord above the level of tortuosity was obtained. Then the transducer was moved down along the cord, and a rotation of the cord structures was looked for. If an acute rotation was seen, it was taken as a positive whirlpool sign. The location of the whirlpool sign and the axis of rotation were noted. If it was not seen, the same maneuver was repeated in all possible angles of the tortuous cord. The gray scale features of the testis and epididymis were studied. If a hydrocele was present, its nature was noted. Then the same technique was repeated with color Doppler sonography. Spectral tracing was done in appropriate situations. The same procedure was repeated on the opposite side. Those patients who did not have surgery underwent laboratory investigations.

Results

During the study period, there were 221 patients with acute scrotal pain. An overview of the diagnoses and the numbers of the cases is given in Table 1⇓.

Table 1.

Sonographic Diagnoses

Diagnosis	No. of patients
Acute epididymo-orchitis	65
Testicular abscess	3
Torsion of appendage of testis	23
Acute idiopathic scrotal edema	19
Complete torsion of testis	61
Incomplete torsion of testis	4
Segmental infarction of testis	9
Torsion-detorsion with hyperemia	1
Equivocal features	14

Diagnosis	No. of patients
Complicated hydrocele	1
Mumps orchitis	1
Henoch-Schönlein purpura vasculitis	1
Normal	5
Lost for follow-up	14
Total	221

There were features characteristic of epididymo-orchitis in 65 patients, including a straight spermatic cord, a swollen epididymis, testis, or both, an absent focal lesion in the testis, with or without a hydrocele, and increased flow on color Doppler studies in the epididymis and testis or epididymis alone associated with clinical and laboratory features of infection or urinary tract infection, such as fever, dysuria, and leukocytosis. The disease involved the right testis in 39 (60%) patients and the left testis in 26 (40%). The age of the patients ranged from 5 months to 76 years. Four of the 65 patients underwent surgical exploration and were confirmed to have epididymo-orchitis. The rest were treated appropriately. They were followed with clinical examination or sonography or by telephone conversation with the patient or his parents after a minimum of 8 weeks in patients with a good response and as required by clinical condition in others. During follow-up, there were testicular or epididymal abscesses in 18 patients, which were treated appropriately. All the other patients were confirmed to have normal-sized testis after 8 weeks.

Three patients in this series with scrotal pain and high fever had testicular abscesses. The testis was swollen with a large hypoechoic area. On color Doppler imaging, there was lack of flow in the hypoechoic area, whereas there was increased flow in the rest of the testis and epididymis. They underwent orchidectomy, which confirmed the diagnosis.

The sonographic diagnosis was torsion of the testicular appendage in 23 patients. These patients had a straight spermatic cord and a normal testis. There was a mass of varying size and echo pattern in relation to the head of the epididymis and upper pole of the testis. A minimal hydrocele was present in 16 (76%) patients. On color Doppler study, there was increased flow seen in the testis and epididymis in 8 patients and in the epididymis only in 15 patients. There was no flow seen in the masses in all the patients. The age of the patients ranged from 4.5 to 15 years. Five of them underwent surgical exploration, which revealed torsion of the testicular appendage in 4 and the epididymal appendage in 1. The rest of the patients were treated conservatively and followed clinically or sonographically and were confirmed to have an uneventful recovery.

Nineteen patients had features of acute idiopathic scrotal edema, which revealed a normal testis and edema of the scrotal wall. The age of these patients ranged from 3 days to 10 years.

Complete testicular torsion was seen in 61 patients who had the whirlpool sign in the spermatic cord on real-time gray scale imaging (Video 1) and absent intratesticular flow on color Doppler studies. On a static image, the mass of the whirlpool had the appearance of a doughnut, a target with concentric rings, a snail shell, or a storm on a weather map (Figure 1⇓). The appearance was best seen with the transducer at different angles. The whirlpool sign was seen in a longitudinal scan of the spermatic cord in 12 (20%) patients and in a transverse scan in 20 (32%) patients. The axis was oblique of varying degrees in 29 (48%) patients. The mass of the whirlpool was seen just outside the external ring (Figure 1B⇓), at a varying distance above the testis (Figure 1, C and D⇓), or posterior to the testis (Figure 2⇓ and Table 2⇓). In 1 child of 3 months, the testis was undescended and seen in the inguinal canal. A whirlpool sign was seen close to it (Figure 3⇓). The maximum width of the mass of the whirlpool was 20 mm. The testis and its environment had varying features on the gray scale imaging of the testis, which are summarized in Table 3⇓. On color Doppler studies, there was no flow in the cord distal to the whirlpool and within the testis (Video 2) in 56 patients. In 5 patients, there was flow seen in the proximal part of the mass of the whirlpool and no flow in the distal part and the testis (Figure 4⇓ and Video 3). Ages of these patients were between 3 months and 57 years. The interval between the onset of acute scrotal pain and sonography ranged from 3 hours to 5 days. A history of a previous episode of testicular pain was present in 24 (40%) patients. Eight of these 24 patients had a sonographic diagnosis of epididymo-orchitis during the previous episode. The condition involved the right testis in 14 (23%) patients and the left testis in 47 (77%). Surgical exploration was done in 48 of these patients and confirmed testicular torsion in all of them. In 40, the testis was gangrenous; therefore, ipsilateral orchidectomy and contralateral orchidopexy were done. In 8

patients, the condition of the testis improved on derotation of the cord; therefore, bilateral orchidopexy was done. Contralateral orchidopexy alone was done in 13 patients who reported late. These 13 patients were followed clinically or sonographically and were confirmed to have a decrease in the size of the symptomatic testis, a feature taken as confirmative of torsion.

Table 2. Sonographic Differential Diagnosis of Acute Scrotum

Features of the Whirlpool Sign

Feature	Complete Torsion	Incomplete Torsion
Total, n	61	4
Axis, n		
Longitudinal	12	0
Transverse	20	2
Oblique	29	2
Location, n		
Outside external ring	6	0
Above testis	43	4
Posterior to testis	11	0
Inguinal canal in undescended testis	1	0

Table 3. Sonographic Differential Diagnosis of Acute Scrotum

Gray Scale Features of Torsion

Feature	Complete Torsion	Incomplete Torsion
Total, n	61	4
Whirlpool sign, n	61	4
Size of testis, n		
Swollen	58	4
Smaller	3	0
Echo texture, n		
Uniformly hypoechoic	30	1
Uniformly hypoechoic with echogenic septa	3	0
Uniform echo pattern with hypoechoic septa	5	0
Focal hypoechoic areas	23	3
Axis, n		
Longitudinal	10	0
Transverse	51	4
Hydrocele, n		
Simple	31	2
Septated	5	0

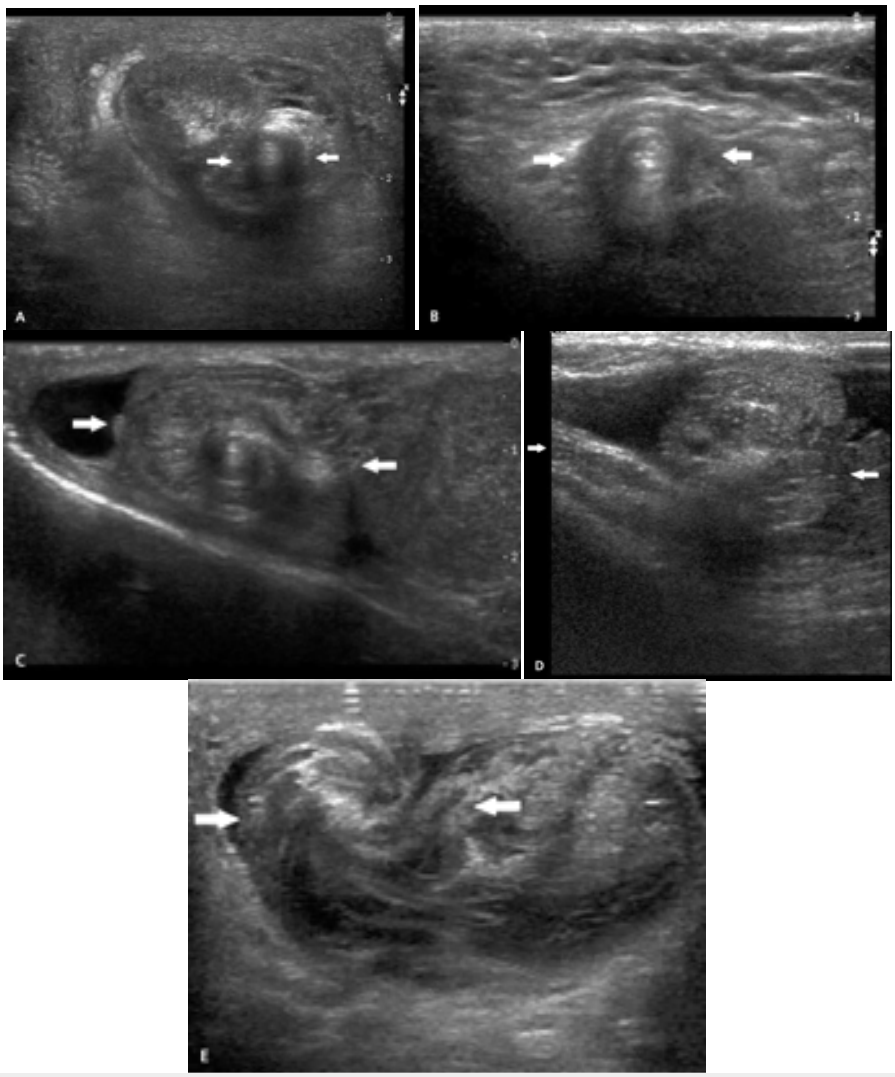

Fig. 1 Various appearances of a whirlpool mass (between arrows) on static images resembling a doughnut (**A**), a target with concentric rings (**B**), a snail shell (**C**), a snail (**D**), and a storm on a weather map (**E**).

Figure 2. Longitudinal scan of a testis in complete torsion showing the testis in the horizontal axis and the whirlpool mass (arrows) posteroinferior to the testis.

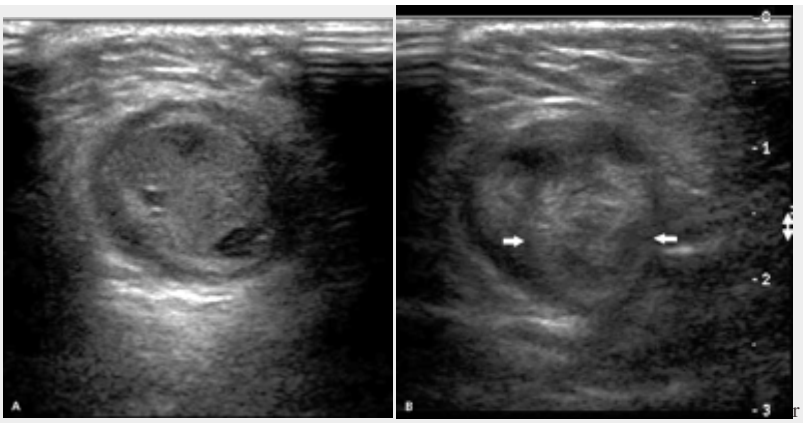

Figure 3. Scans of the left inguinal region showing a swollen and hypoechoic undescended testis in the inguinal canal secondary to torsion (**A**) and a whirlpool mass (arrows) just lateral to the testis (**B**).

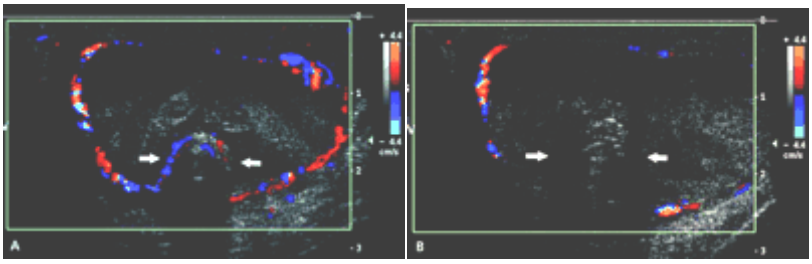

Figure 4. A, Color Doppler image showing the vessels in the proximal part of a whirlpool mass (arrows). **B**, Flow is absent in the distal part of the whirlpool (arrows).

In 4 patients, the whirlpool sign was seen in the mass of the spermatic cord on both gray scale and color Doppler imaging (Figure 5⇓ and Video 4). On color Doppler studies, the visualized vessels were seen to rotate around the central axis. Blood flow was seen in the distal cord, too. In 1 of these patients, the whirlpool sign was seen only on a dynamic real-time study, and a whirlpool mass was not seen on a static image. In these patients, the appearance of the testis was variable. In 1 patient, the testis was swollen and hypoechoic without any focal changes. On a color Doppler study, there were sparse vessels seen in the testis. In the other 3 patients, the testis was swollen and revealed focal hypoechoic areas of varying size. On color Doppler studies, there was no flow seen in the hypoechoic areas, suggestive of segmental infarction. The rest of the testis with a normal echo pattern showed a normal flow pattern in 2 patients and hyperemia in 1. The visualized intratesticular vessels revealed a normal flow pattern on spectral tracing in all 4 patients. These 4 patients underwent surgical exploration. There was torsion of the cord (Figure 5D⇓) in all of them. The testis was swollen with features of ischemia or segmental infarction. After detorsion of the cord, there was improvement in the appearance of the testis; therefore, bilateral orchidopexy was done. In 2 patients, the testis was normal in appearance on follow-up sonography performed 8 weeks later and also on color Doppler studies. On the initial scan, 1 of these 2 patients did not show focal changes, and the other showed hyperemia. In the other 2 patients, the testes had atrophied. These 4 patients were concluded to have partial or incomplete torsion.

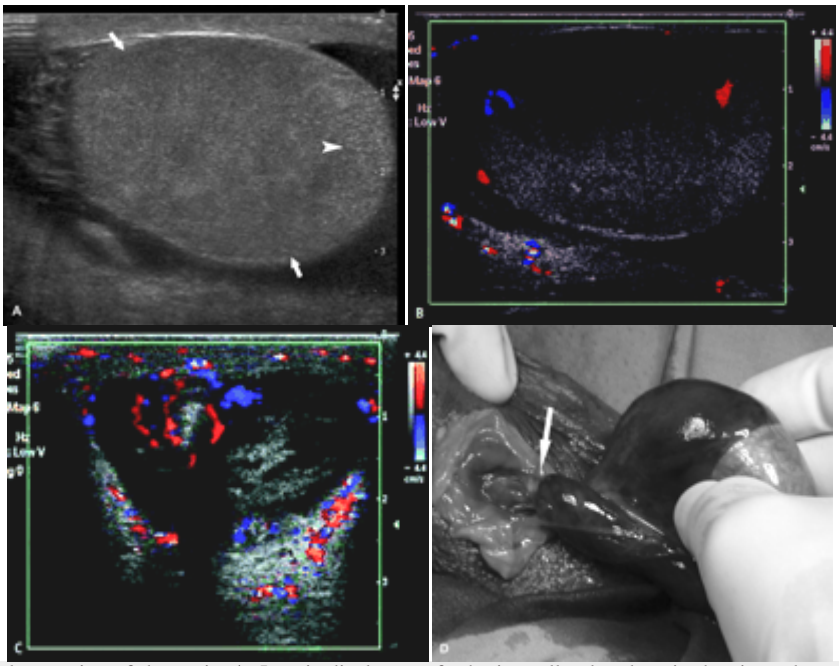

Figure 5. Incomplete torsion of the testis. **A**, Longitudinal scan of a horizontally placed testis showing a large hypoechoic area (arrows) in the upper two thirds of the testis and a normal echo pattern (arrowhead) in the lower third. **B**, Color Doppler image showing no flow in the hypoechoic area with a few vessels seen in the poles. **C**, Color Doppler image of the whirlpool mass showing the visualized vessels going around the central axis. **D**, Ischemic testis with the segmental infarction of the upper two thirds and torsion of the spermatic cord (arrow).

In 9 patients, the spermatic cord was straight, and the axis of the testis was horizontal. The testis was swollen in 8 of them and smaller in 1. The testis revealed hypoechoic lesions of varying size. On color Doppler studies, there was no detectable flow in these hypoechoic areas. The area of the testis with the normal echo pattern revealed a normal arterial flow pattern in 7 patients and hyperemia in 2 (Figure 6⇓). The epididymis was either normal or increased in size and showed increased flow on color Doppler studies in all these patients. In 1 patient, there was wide separation of testis and epididymis, suggestive of a long mesorchium. All these patients gave a history of acute testicular pain of varying but short durations, which was spontaneously relieved. They were free of symptoms for 5 hours to 10 days before scanning. None of them had fever or evidence of conditions associated with vasculitis. All these patients underwent surgical exploration, and the testis was swollen in 8 and normal in size in 1. All the testes revealed ischemic regions of various sizes suggestive of segmental infarction of the testis (Figure 6D⇓). In 1 patient, a long mesorchium was confirmed. On needle prick, there was a subnormal bleeding response. Orchidectomy with contralateral orchidopexy was done in 7 patients. Histopathologic examination confirmed segmental hemorrhagic infarction in all of them. In 2 patients, bilateral orchidopexy was done. On follow-up, both of them had a decrease in the size of the testis. In all these patients, the features seen in the testis were suggestive of segmental infarction of the testis. None of them proved to have a preexisting vascular disease to explain the infarction. All the patients gave a history of acute testicular pain of short duration with spontaneous relief. The testis was placed horizontally in all of them. Because of all these features, the patients in this group were concluded to have segmental testicular infarction due to a torsion-spontaneous detorsion sequence or ITT.

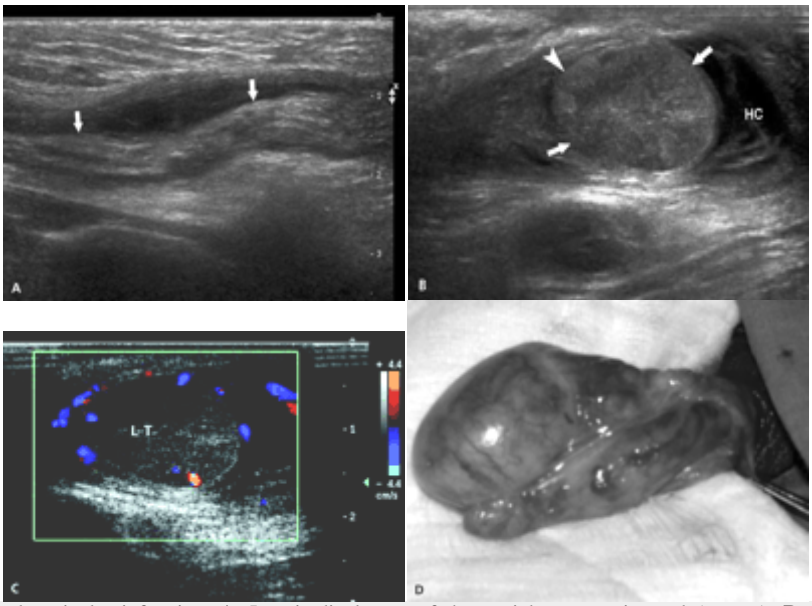

Figure 6. Segmental testicular infarction. **A**, Longitudinal scan of the straight spermatic cord (arrows). **B**, Longitudinal scan showing a transverse section of a swollen testis with a large hypoechoic area (arrows) in the lower part and a normal echo pattern (arrowhead) in the upper part. There is a septated hydrocele (HC). **C**, Color Doppler image showing lack of flow in the hypoechoic area with a few vessels in the periphery of the left testis (LT). **D**, Ischemic testis with segmental infarction.

One patient aged 23 years gave a history of 3 attacks of acute left testicular pain lasting for 5 to 10 minutes with spontaneous relief of pain starting from the age of 8 years. He sought care 6 hours after the most recent episode. He did not have a fever. On sonography, the spermatic cord was straight. The testis was placed along the horizontal axis. The testis and epididymis showed subtle increases in size with decreased echogenicity, which could be recognized only on meticulous comparison with the contralateral testis. On a color Doppler study, there was unequivocal increased flow seen in the left testis and epididymis (Figure 7⇓). It was concluded to be a torsion-detorsion sequence. Bilateral orchidopexy was done after 1 month, at which time both the testes were normal.

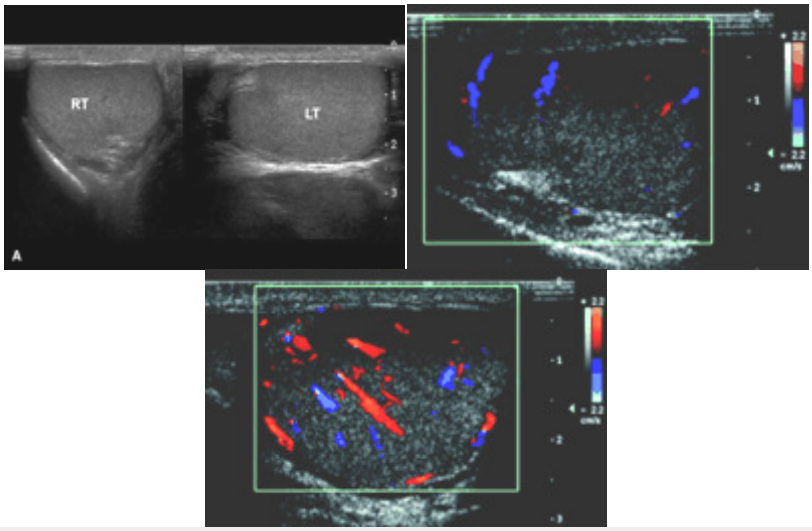

Figure 7. Intermittent testicular torsion. **A**, Transverse scan of a **scrotum** showing the short axis of the right testis (RT) and long axis of the left testis (LT) indicating the horizontally placed left testis. The left testis is slightly hypoechoic compared with the right testis. **B**, Color Doppler image of the right testis showing a normal flow pattern. **C**, Color Doppler image showing increased flow in the left testis.

Fourteen children had acute **scrotum** without fever. Sonography revealed a straight spermatic cord and a swollen testis and epididymis. On color Doppler studies, there was unequivocal increased flow in the testis and epididymis. They did not have evidence of infection or urinary tract infection. They were treated with antibiotics. Twelve of them had a normal-sized testis after 8 weeks. These patients could have had either epididymo-orchitis or ITT. In 2 of these 14 patients, the testis had atrophied, indicating that they most probably had ITT.

There was a complicated hydrocele alone in 1 patient. In 2 patients, there were preceding illnesses of mumps and Henoch-Schönlein purpura. In both patients, sonography showed a swollen, hypoechoic testis with hyperemia, suggestive of orchitis due to these etiologies. Sonographic findings were normal in 5 patients. Fourteen patients were lost for follow-up.

Discussion

Acute scrotal pain can have diverse causes. The most important objective of treatment of these patients is to rule in or rule out testicular torsion. It requires immediate intervention to avoid infarction of the affected testis.[19] Conversely, if torsion can be confidently ruled out, unnecessary surgical intervention can be avoided. Intermittent testicular torsion or a torsion-detorsion sequence is a clinical syndrome defined by a history of unilateral scrotal pain of sudden onset and of short duration that resolves spontaneously.[15] The natural history of ITT varies. Some patients may have acute torsion at a later date. This is evidenced by the observation that up to half of patients with acute torsion report previous episodes of testicular pain.[3] In this series, the incidence of previous episodes was 40%. Some patients have continued attacks, which, if lasting enough, can result in ischemic damage to the testis, although definite evidence of this is lacking.[4,16,18]

Currently, a sonographic study of acute **scrotum** is focused on evaluation of the testis, epididymis, and scrotal wall on gray scale sonography and study of the intratesticular vascular flow by color Doppler imaging.[9–12,14,20–23] However, there are situations that may show inconclusive results on color Doppler studies. The torsion-detorsion phenomenon may show testicular hyperemia, mimicking an inflammatory process.[23,24] There are reports of spermatic cord torsion with preserved testis perfusion on color Doppler studies.[11,25–28] Arce et al[13] and Baud et al[14] concluded that all these pitfalls occur because of indirect evaluation of a condition that is caused elsewhere, and they proposed to study the spermatic cord directly because actual torsion occurs there. Baud et al[14] and Kalfa et al[29] studied the spermatic cord in its entire length, including the inguinal canal, and described a spiral twist of the cord at the external inguinal ring diagnostic of torsion, irrespective of the color Doppler findings in the testis. They described high sensitivity and specificity of this sign. The rate of unnecessary surgery was 0%. The same sign was elicited in this series with a real-time modification in the form of downward movement of the transducer along the spermatic cord to look for the whirlpool sign. The mass of torsion of the cord had the appearance of a doughnut, a target, a snail shell, or a storm on a weather map. The movement of the transducer in a downward direction perpendicular to the axis of this mass brought on the whirlpool sign. The whirlpool mass is seen in various locations: just distal to the external ring, above the testis or posterior to the testis, and in the inguinal canal if the testis is undescended. The angle at which it is best seen also varies. This sign was seen in 65 patients in this series, all of whom were proved to have testicular torsion, complete in 61 and incomplete in 4. In complete torsion, the whirlpool sign is seen only on gray scale sonography with absent intratesticular flow on color Doppler imaging. In incomplete torsion, there is flow in the vessels of the whirlpool mass, distal to it, and in the testis. The whirlpool sign is seen on gray scale as well as color Doppler imaging. The incomplete torsion probably explains the cases reported in earlier reports as missed torsion or torsion with preserved testicular perfusion, and the whirlpool sign helps in diagnosis of torsion in such patients. Hence, the real-time whirlpool sign is the most definitive sign of torsion because it has 100% specificity and sensitivity; there were no false-positive or -negative findings of torsion in this series.

The second group of patients has a straight spermatic cord, a swollen testis, epididymis, or both, absent focal changes in the testis, and unequivocal increased flow in the testis and epididymis. Sometimes the flow may be increased in the epididymis alone with normal flow in the testis. These features may be seen in either acute epididymo-orchitis or ITT,[5] and the differentiation is based on the presence or absence of clinical or laboratory evidence of infection.[5] Patients with acute epididymo-orchitis have some clinical features suggestive of epididymo-orchitis, such as fever, dysuria, and laboratory evidence of leukocytosis or urinary tract infection, seen in 65 patients in this series. The patients with ITT lack these clinical features of epididymo-orchitis, and instead they may give a typical history of acute pain of short duration with spontaneous relief, which is usually associated with vomiting. The axis of the testis is horizontal. We had 1 patient with this diagnosis. The finding of epididymal or testicular hyperemia or both in ITT is indicative of reactive hyperemia and is seen in 17% of patients with ITT. A consistent sonographic sign described in ITT is the horizontal lie of the testis.[5]

In 14 children in this series, who had a straight spermatic cord and hyperemia, a diagnosis could not be offered because there was lack of any differentiating clinical or laboratory features. The usefulness of the horizontal testicular axis in ITT[5] was not yet known during that period of study; hence, the observation was not looked for in those patients. This observation may be a useful sonographic sign in such patients.

The fourth group has a straight spermatic cord, a horizontally oriented testis, a swollen testis and epididymis, focal changes in the testis, and increased flow in the spermatic cord and epididymis with decreased or increased flow in the testis. The focal hypoechoic areas in the testis lack blood flow on color Doppler imaging. The possible diagnoses in these patients are segmental infarction (due to ITT or vasculitis) and epididymo-orchitis

with suppuration of the testis. The differentiation is by clinical or laboratory evidence of infection for a testicular abscess and the lack of such evidence with a horizontal axis of the testis for ITT.[30] In this series, there were 12 patients with these features, and 9 of them turned out to have ITT with segmental infarction and 3 to have testicular abscesses.

There was no case of unnecessary surgery in this series (0%). There were only 2 cases of missed torsion in this series of 207 patients (1%) who were followed for at least 8 weeks, which included all forms of torsion. These 2 patients had equivocal sonographic features with testicular hyperemia. The limitation of the study is that the patients with acute epididymo-orchitis (65 cases) and those with testicular or epididymal hyperemia who were not given a sonographic diagnosis (14 cases) were followed for a period of 8 weeks only, which is short considering the possibility of ITT occurring after a gap of even years. Follow-up extending for more time is not possible in the health care system existing in this country. The length of follow-up, however, would form a good subject of study in a society with a closed health care system, where patients could be followed for many years; that would give the true incidence of ITT versus acute epididymo-orchitis in the presence of testicular or epididymal hyperemia.

From the data of this series and those of recent publications, one can draw the following conclusions about ITT. The sonographic features of this syndrome will depend on the time between sonography and the event, the severity of the torsion, and the duration of the event. If the patient reports after a few days of a mild event, the sonographic findings may be normal. If he reports within a few hours after severe torsion and complete detorsion, the testis would be slightly swollen and hypoechoic, and the spermatic cord would be straight. There would be hyperemia of the testis on color Doppler imaging. The same features are also seen in acute epididymo-orchitis. The differentiation of ITT and epididymo-orchitis in this situation is only clinical. One useful and consistent sonographic finding in ITT is the horizontal lie of the testis.[3,5] Some of these patients with a torsion-detorsion sequence showing testicular hyperemia and mimicking epididymo-orchitis have testicular atrophy later, which is well documented.[16] It was seen in 2 patients in this series. Eight patients in this series who had classic features of acute torsion had reports of an earlier sonographic diagnosis of acute epididymo-orchitis because of testicular hyperemia, indicating that they had a torsion-detorsion sequence on the previous occasion, which also corroborates this phenomenon.

The third group of the patients with ITT, who have severe torsion with complete detorsion and report early, reveal sonographic features of segmental testicular infarction.[30] The horizontally placed testis reveals focal hypoechoic areas that lack blood flow, with the rest of the testis showing a normal echo pattern. These areas with a normal echo pattern either show normal blood flow in sparse arteries or show hyperemia. The epididymis may show increased blood flow. Although polycythemia, sickle cell anemia, and acute angitis have been linked to segmental infarction, the cause of most reported cases is unknown,[30–33] and these were probably in fact cases of ITT. The differential diagnosis of this condition can be severe orchitis with suppuration. The differentiation of these conditions is by the clinical features of infection seen in epididymo-orchitis and the history of acute pain with spontaneous relief, a history of a previous episode, and a horizontal testicular axis in ITT.

In conclusion, testicular torsion is a complex condition with a spectrum of clinical and sonographic features. In complete torsion, there is a whirlpool sign on gray scale sonography and absence of flow in the distal cord, testis, and epididymis. In incomplete torsion, there is a whirlpool sign on gray scale and color Doppler sonography and varying amounts of vessels within the testis. The sonographic real-time whirlpool sign is the most specific sign of torsion, either complete or incomplete, because it reveals the actual anomaly. Alternatively, the torsion may present a challenging spectrum of clinical features that may be due to ITT. The symptoms are acute onset of severe scrotal pain with spontaneous relief after a short time. The sonographic spectrum of this condition varies depending on the severity and duration of the event and the time between the event and sonography. There may be features of segmental testicular infarction, testicular hyperemia, or a normal testis.

The following algorithm is suggested for sonography in a case of acute scrotal pain:

1. When the clinical history and physical examination are sufficiently alarming and unequivocal for testicular torsion and sonography is not possible immediately, surgical exploration is done without any imaging.

2. When there are unequivocal sonographic features of the following conditions, the patient is treated accordingly: testicular torsion showing total absence of intratesticular blood flow, torsion of the testicular appendage, and acute idiopathic scrotal edema.

3. When there is symmetric or asymmetric arterial flow seen in the testis, the spermatic cord is studied in detail to look for the whirlpool sign. The real-time whirlpool sign is the most specific sign of both complete and incomplete testicular torsion.

4. Features of segmental testicular infarction and a horizontal lie of the testis in a patient without features of systemic vascular disease or infection are diagnostic of ITT. Prophylactic contralateral orchidopexy should be performed to preserve the normal testis because of the high association of future contralateral torsion.

5. In a case with features of a straight cord and a swollen testis and epididymis with hyperemia, acute epididymo-orchitis and ITT are both possible. The diagnosis of acute epididymo-orchitis is made when there are clinical or laboratory features of infection or urinary tract infection. A history of pain with spontaneous relief and a horizontal testicular axis indicate ITT. When these differentiating features are absent, the patients need active follow-up. This is essential because ITT is a possibility. The challenges of clinical decision making in these patients lie in the recognition that there is no definitive diagnostic test to confirm ITT. Only by halting the pattern of recurrent pain can the diagnosis be made, albeit retrospectively.[18] When there is a clinical history typical of ITT and a horizontal testicular axis, bilateral orchidopexy is done immediately.

References

1. ↵
Williamson RC. Torsion of the testis and allied conditions. Br J Surg 1976; 63:465–476.
Medline

2. ↵
Caesar RE, Kaplan GW. Incidence of the bell-clapper deformity in an autopsy series. Urology 1994; 44:114–116.
CrossRefMedline

3. ↵
Kamaledeen S, Surana R. Intermittent testicular pain: fix the testes. BJU Int 2003; 91:406–408.
Medline

4. ↵
Schulsinger D, Glassberg K, Strashun A. Intermittent torsion: association with horizontal lie of the testicle. J Urol 1991; 145:1053–1055.
Medline

5. ↵
Eaton SH, Cendron MA, Estrada CR, et al. Intermittent testicular torsion: diagnostic features and management outcomes. J Urol 2005; 174:1532–1535.
CrossRefMedline

6. ↵
Krarup T. The testes after torsion. Br J Urol 1978; 50:43–46.
Medline

7. *Chakraborty J, Hikim AP, Jhunjhunwala JS. Quantitative evaluation of testicular biopsies from men with unilateral torsion of spermatic cord. Urology 1985; 25:145–150.*
Medline

8. ↵
Skoglund RW, McRoberts JW, Ragde H. Torsion of the spermatic cord: a review of the literature and an analysis of 70 new cases. J Urol 1970; 104:604–607.
Medline

9. ↵
Burks DD, Markey BJ, Burkhard TK, Balsara ZN, Haluszka MM, Canning DA. Suspected testicular torsion and ischemia: evaluation with color Doppler sonography. Radiology 1990; 175:815–821.
Abstract/FREE Full Text

10. *Paltiel HJ, Connolly LP, Atala A, Paltiel AD, Zurakowski D, Treves ST. Acute scrotal symptoms in boys with an indeterminate clinical presentation: comparison of color Doppler sonography and scintigraphy. Radiology 1998; 207:223–231.*
Abstract/FREE Full Text

11. ↵

Kravchick S, Cytron S, Leibovici O, et al. Color Doppler sonography: its real role in the evaluation of children with highly suspected testicular torsion. Eur Radiol 2001; 11: 1000–1005.
CrossRefMedline

12. ↵
Aso C, Enriquez G, Fite M, et al. Gray-scale and color Doppler sonography of scrotal disorders in children: an update. Radiographics 2005; 25:1197–1214.
Abstract/FREE Full Text
13. ↵
Arce JD, Cortes M, Vargas JC. Sonographic diagnosis of acute spermatic cord torsion. Rotation of the cord: a key to the diagnosis. Pediatr Radiol 2002; 32:485–491.
CrossRefMedline
14. ↵
Baud C, Veyrac C, Couture A, Ferran JL. Spiral twist of the spermatic cord: a reliable sign of testicular torsion. Pediatr Radiol 1998; 28:950–954.
CrossRefMedline
15. ↵
Creagh TA, McDermott TE, McLean PA, Walsh A. Intermittent torsion of the testis. BMJ 1988; 297:525–526.
FREE Full Text
16. ↵
Sellu DP, Lynn JA. Intermittent torsion of the testis. J R Coll Surg Edinb 1984; 29:107–108.
Medline
17. ↵
Blumberg JM, White B, Khati NJ, Andrawis R. Intermittent testicular torsion in a 58-year-old man. J Urol 2004; 172: 1886.
Medline
18. ↵
Stillwell TJ, Kramer SA. Intermittent testicular torsion. Pediatrics 1986; 77:908–911.
Abstract/FREE Full Text
19. ↵
*Kass EJ, Stone KT, Cacciarelli AA, Mitchell B. Do all children with an acute **scrotum** require exploration? J Urol 1993; 150:667–669.*
Medline
20. ↵
Patriquin HB, Yazbeck S, Trinh B, et al. Testicular torsion in infants and children: diagnosis with Doppler sonography. Radiology 1993; 188:781–785.
Abstract/FREE Full Text
21. *Middleton WD, Middleton MA, Dierks M, Keetch D, Dierks S. Sonographic prediction of viability in testicular torsion: preliminary observations. J Ultrasound Med 1997; 16:23–27.*
Abstract
22. *Wilbert DM, Schaerfe CW, Stern WD, Strohmaier WL, Bichler KH. Evaluation of the acute **scrotum** by color-coded Doppler ultrasonography. J Urol 1993; 149:1475–1477.*
Medline
23. ↵
Middleton WD, Siegel BA, Melson GL, Yates CK, Andriole GL. Acute scrotal disorders: prospective comparison of color Doppler US and testicular scintigraphy. Radiology 1990; 177:177–181.
Abstract/FREE Full Text
24. ↵
*Ralls PW, Larsen D, Johnson MB, Lee KP. Color Doppler sonography of the **scrotum**. Semin Ultrasound CT MR 1991; 12:109–114.*
Medline
25. ↵
Bentley DF, Ricchiuti DJ, Nasrallah PF, McMahon DR. Spermatic cord torsion with preserved testis perfusion: initial anatomical observations. J Urol 2004; 172:2373–2376.
CrossRefMedline
26. *Steinhardt GF, Boyarsky S, Mackey R. Testicular torsion: pitfalls of color Doppler sonography. J Urol 1993; 150:461–462.*
Medline

27. *Allen TD, Elder JS. Shortcomings of color Doppler sonography in the diagnosis of testicular torsion. J Urol 1995; 154:1508–1510.*
CrossRefMedline

28. ↵
Ingram S, Hollman AS, Azmy A. Testicular torsion: missed diagnosis on colour Doppler sonography. Pediatr Radiol 1993; 23:483–484.
CrossRefMedline

29. ↵
Kalfa N, Veyrac C, Baud C, Couture A, Averous M, Galifer RB. Ultrasonography of the spermatic cord in children with testicular torsion: impact on the surgical strategy. J Urol 2004; 172:1692–1695.
CrossRefMedline

30. ↵
Ledwidge ME, Lee DK, Winter TC III, Uehling DT, Mitchell CC, Lee FT Jr. Sonographic diagnosis of superior hemispheric testicular infarction. AJR Am J Roentgenol 2002; 179:775–776.
FREE Full Text

31. *Costa M, Calleja R, Ball RY, Burgess N. Segmental testicular infarction. BJU Int 1999; 83:525.*
CrossRefMedline

32. *Baratelli GM, Vischi S, Mandelli PG, Gambetta GL, Visetti F, Sala EA. Segmental hemorrhagic infarction of testicle. J Urol 1996;156:1442.*
CrossRefMedline

33. ↵
Bird K, Rosenfield AT. Testicular infarction secondary to acute inflammatory disease: demonstration by B-scan ultrasound. Radiology 1984; 152:785–788.

4º caso: foi comentado sobre **HIDROCELES.** O autor menciona que 15% dos fetos tem hidroceles e a maioria delas são não comunicantes. O autor mostrou então caso de hidrocele do escroto ao canal inguinal, denominada abdominoescrotal, que é uma condição rara e onde a coleção líquida vai da bolsa escrotal até o abdome através do canal inguinal.

5º caso: um paciente de 3 anos com escroto aumentado e dor, cuja hipótese principal era torção. Entretanto, o exame US + Doppler demonstrou que não havia torção, mas a parede escrotal estava muito espessada, difusamente hipoecóica. Não havia explicação US para esse achado e o questionário clínico revelou que o paciente era portador de síndrome nefrótica, ou seja, apenas a parede escrotal estava edemaciada.

6º caso: no diagnóstico diferencial da dor testicular deve-se considerar a hipótese de hematocele pós trauma (chute testicular é bastante frequente como fator etiológico) e a fratura testicular. Neste caso as margens devem estar irregulares indicando a ruptura/fratura. É importantíssimo diagnosticar esses casos, pois eles requerem cirurgia imediata de urgência. Nos casos de hematoma o testículo está aumentado, heterogêneo, com áreas hipo e hiperecogênicas amorfas esparsas e áreas císticas irregulares entremeadas.

7º caso: mostrou caso de um paciente com leucemia previamente tratada e recidivada. A imagem mostra o testículo difusamente hipoecóico e hipervascularizado. Na recidiva da leucemia é comum o comprometimento testicular, o que não ocorre na fase inicial da moléstia.

8º caso: mostrou um paciente com microlitíase testicular, com calcificações de 1 a 3 mm esparsas difusamente pelo testículo. Este quadro tem prevalência de 0.6% e está associado ao aumento da incidência de tumor testicular, o qual é mais frequente se a calcificação testicular for isolada.

A segunda apresentação foi de Regina Hooley, MD, assistant professor of Yale university, que expôs o tema da **DOR PÉLVICA AGUDA** . Esta aula abordou vários casos:

1º caso: um caso de dor pélvica aguda em uma jovem de 25 anos com dor aguda no baixo ventre que apresentava ruptura de cisto hemorrágico e hematoperitôneo.

2º caso: outro caso de dor pélvica aguda em uma jovem de 25 anos, com BHCG positivo, que correspondia a gestação ectópica (GE). Nos casos de GE o diagnóstico é realizado quando o US detecta SG ou embrião extra uterino, sendo comum a associação com líquido livre peritoneal com partículas sólidas em suspensão. Nos casos de suspeita de gestação cervical, é importantíssimo fazer o diagnóstico diferencial com abortamento em curso. Trata-se de GE cervical somente se o exame Doppler detectar fluxo nos trofoblastos ou no embrião, caso

contrário a hipótese preferencial é de abortamento em curso. Recomendou que o tratamento com metrotrexate da GE deve conter certos critérios, sendo o principal deles a estabilidade hemodinâmica. Outros critérios incluem:

- estar absolutamente certo de que é GE
- excluir gestação gemelar normal precoce (elevam muito os níveis do BHCG e dá reação cruzada com o valor de corte para suspeita de GE) associada a ruptura de corpo lúteo.
- Excluir gestação gemelar heteróloga (tópica e ectópica concomitantemente), cuja incidência está aumentando com as FIVs

3º caso: mostrou caso de gestação anembrionária. Recomenda que para o diagnóstico de gestação anembrionária se utilize o novo valor de corte, que é SG maior que 25mm, com ou sem saco vitelino (antigo valor de corte era: SG > 8mm com saco vitelino ou SG > 16mm sem embrião). O antigo valor de corte estava dando alguns falsos negativos que evoluíram para gestação normal. O critério para aborto é CCN maior que 7mm sem atividade cardíaca (antigo valor de corte era CCN maior que 5 – 6mm, sem atividade cardíaca com BHCG > 2000 UI). Mostrou um caso de uma moça de 24 anos com sangramento vaginal e BHCG positivo e gestação de localização desconhecida no rastreamento US. Esta é uma ocorrência comum, detectada em 8 a 31% dos consultórios US, que decorre de quão precoce é a gestação quando se interroga a possibilidade de GE. A maioria desses casos são abortos, mas é fundamental observar:

- Se é gestação tópica o BHCG aumenta normalmente;
- Se é aborto o BHCG reduz gradualmente;
- Se é GE o BHCG permanece num platô.

4º caso: mostrou caso de uma mulher de 43 anos com dor pélvica à esquerda cujo diagnóstico foi de torção de ovário. Este diagnóstico ocorre em mais de 3% dos casos de emergência ginecológica, sendo o lado direito mais comumente afetado do que o esquerdo. Um dos principais fatores de risco é a presença de massa anexial maior que 5cm, que favorece a torção. No US observa-se, como **sinais principais da torção gonadal**:

- a presença de múltiplos cistos gonadais periféricos;
- hipoecogenicidade difusa da região central do ovário;

  Os **achados Doppler da torção gonadal** são muito variáveis, sendo os principais, em ordem progressiva de gravidade:
- fluxo detectável é apenas o arterial, pois o venoso é obstruído mais precocemente;
- fluxo apenas no pedículo vascular do ovário (sinal do turbilhão ou Whirlpool)
- ausência completa de fluxo.

A sessão da tarde de 30/03/2012 incluiu palestras sobre **OS AVANÇOS DA ULTRASSONOGRAFIA MÚSCULO ESQUELÉTICA**, moderada por Levon Nazarian.

A primeira palestra foi sobre **IMAGEM FUNDIDA: CT/RNM COM US PARA PROCEDIMENTOS DE DIRECIONAMENTE**, ministrada por Joseph Craig, radiologista do Henry Ford Hospital, Detroit. A aula fez uma revisão sobre uma nova técnica de diagnóstico por imagem, a fusão da imagem seccional da RNM e CT com os dados ultrassonográficos. Nesta técnica os dados da CT ou RNM são fundidos com o exame ultrassonográfico usando pontos de registro fixados. Na imagem US dinâmica os dados do CT ou RNM do mesmo plano são mostrados na tela do equipamento de US. O equipamento US de fusão é equipado com um emissor de rádio freqüência e a sonda US é equipada com um sensor de posição, para poder interpretar corretamente a topografia das imagens equivalentes de RNM e CT. Desta forma o equipamento de US tem a capacidade de fundir as três informações, o que é particularmente útil na biópsia do sistema músculo esquelético, em especial quando a biópsia do tecido ósseo deve ser realizada concomitantemente com as tecidos de partes moles. Os autores comentam que quando a massa é excessivamente pequena torna-se difícil a fusão das imagens dos três métodos de forma adequada. Esta tecnologia foi inicialmente para um sensor de posição duplo implantado numa sonda de US.

Esquemas da sonda US para imagem de fusão

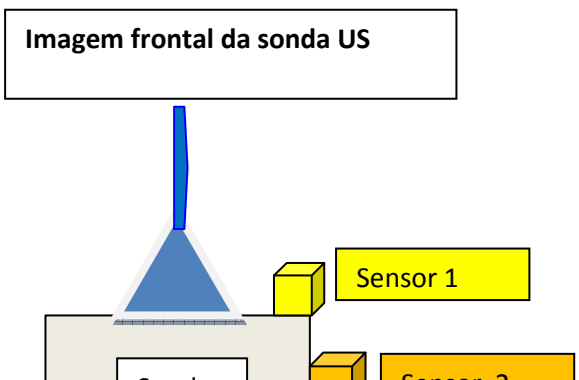

Imagem perfil da sonda US de fusão

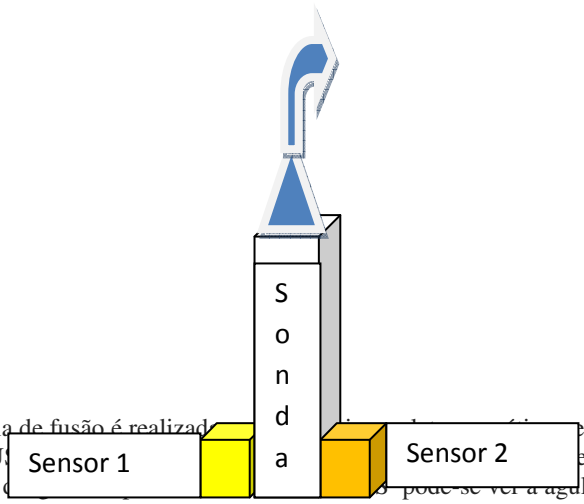

A biópsia de fusão é realizad[illegible]erto do paciente, enquanto o exame é realizado com o U[illegible]e elas são adicionadas em arquivo do US para ajudar a [illegible] pode-se ver a agulha movimentando-se em tempo real, mas não há radiação para o paciente ou operador. A principal contra indicação é a exposição a um campo eletromagnético, embora de baixa intensidade. Esta tecnologia incorpora as varreduras de CT ou RNM previamente realizadas e quando se direciona a agulha para o alvo, é possível seguir com a ultrassonografia em tempo real. O autor mostrou uma biópsia de osteossarcoma realizado com o sistema e outra biópsia de uma metástase óssea de carcinoma pulmonar que estava destruindo a tíbia e invadindo os tecidos de partes moles adjacentes. Entre as principais limitações e problemas é o tempo de aprendizado e registro, que é bastante demorado. É necessário que o registro seja perfeito para fazer a fusão dos três métodos de imagem, principalmente se a lesão for pequena e profunda. Caso contrário, pode-se perdê-la na biópsia. Pode-se perder o alvo da biópsia caso a paciente se mexa durante o procedimento de registro e ter que recomeçar todo o procedimento novamente.
O autor conclui que é uma técnica em desenvolvimento que precisa ser aprimorada, mas que permite realizar biópsias profundas e intraósseas com a técnica de fusão das imagens US, RNM e CT.

A segunda palestra foi sobre **ELASTOGRAFIA: APLICAÇÕES EM MÚSCULOESQUELÉTICO**, ministrada por Levon Nazarian. O autor citou as novas aplicações da elastografia músculo esquelética, em especial uma técnica nova que tem a possibilidade de detectar pontos de gatilho pela fibroelastografia, conforme publicado recentemente em outubro de 2011 no Journal of Ultrasound in Medicine:

Objective Sonographic Measures for Characterizing Myofascial Trigger Points Associated With Cervical Pain

Jeffrey J. Ballyns, PhD, Jay P. Shah, MD, Jennifer Hammond, BS, Tadesse Gebreab, BS, Lynn H. Gerber, MD and Siddhartha Sikdar, PhD⇓

Abstract

Objectives— The purpose of this study was to determine whether the physical properties and vascular environment of active myofascial trigger points associated with acute spontaneous cervical pain, asymptomatic latent trigger points, and palpably normal muscle differ in terms of the trigger point area, pulsatility index, and resistivity index, as measured by sonoelastography and Doppler imaging.

Methods— Sonoelastography was performed with an external 92-Hz vibration in the upper trapezius muscles in patients with acute cervical pain and at least 1 palpable trigger point (n = 44). The area of reduced vibration amplitude was measured as an estimate of the size of the stiff myofascial trigger points. Patients also underwent triplex Doppler imaging of the same region to analyze blood flow waveforms and calculate the pulsatility index of blood flow in vessels at or near the trigger points.

Results— On sonoelastography, active sites (spontaneously painful with palpable myofascial trigger points) had larger trigger points (mean ± SD, 0.57 ± 0.20 cm^2) compared to latent sites (palpable trigger points painful on palpation; 0.36 ± 0.16 cm^2) and palpably normal sites (0.17 ± 0.22 cm^2; $P < .01$). Analysis of receiver operating characteristic curves showed that area measurements could robustly distinguish between active, latent, and normal sites (areas under the curve, 0.9 for active versus latent, 0.8 for active versus normal, and 0.8 for latent versus normal, respectively). Doppler spectral waveform data showed that vessels near active sites had a significantly higher pulsatility index (median, 8.3) compared to normal sites (median, 3.0; $P < .05$).

Conclusions— The results presented in this study show that myofascial trigger points may be classified by area using sonoelastography. Furthermore, monitoring the trigger point area and pulsatility index may be useful in evaluating the natural history of myofascial pain syndrome.

color Doppler imaging, elastography, myofascial trigger points, sonography

Myofascial pain syndrome is a substantial health problem in the United States, believed to affect about 23 million Americans.[1] Myofascial pain syndrome is a very common, complex, yet poorly understood form of neuromuscular dysfunction consisting of motor and sensory abnormalities. It is a major progenitor of nonarticular local musculoskeletal pain and tenderness that affects every age group and is commonly recognized as "muscle knots."[2] Myofascial pain syndrome is associated with numerous pain conditions, including radiculopathies, joint dysfunction, disk abnormalities, tendonitis, and many others.[3] It is characterized by myofascial trigger points, which are discrete hypersensitive hard palpable nodules located within taut bands of contractured skeletal muscle. Myofascial trigger points can be found by palpation of the soft tissue performed by a trained examiner and are painful on compression. The local twitch response is an important clinical finding that confirms the presence of a trigger point. The local twitch response is a quick, localized contraction of muscle fibers produced by strumming or snapping the taut band in a direction perpendicular to the muscle fibers. Trigger points are classified clinically as active or latent.[4] An active myofascial trigger point causes spontaneous pain and may often cause general motor dysfunction (stiffness and restricted range of motion). A latent myofascial trigger point often causes motor dysfunction without pain. Pain associated with latent myofascial trigger points requires firm palpation or a mechanical stimulus to elicit.[5] Otherwise, latent myofascial trigger points have all of the characteristics of active myofascial trigger points, although usually to a lesser degree.[3,6]

Although the specific pathophysiologic basis of myofascial trigger point development and symptoms is unknown, several promising lines of scientific study (ie, histologic, neurophysiologic, biochemical, sonographic, and somatosensory) have revealed objective abnormalities.[7–13] Furthermore, our group has found that differences among active, latent, and normal sites may be evaluated objectively using diagnostic sonographic techniques, such as gray scale (2-dimensional) sonography, vibration sonoelastography, and Doppler imaging.[12]

Most of the investigational work on myofascial pain secondary to myofascial trigger points has involved human patients because no successful animal model has been found to elucidate how these nodules arise or how to treat them in a controlled setting. Furthermore, there are very few studies describing objective and clinically applicable methods for identifying and classifying myofascial trigger points. The few that do exist have attempted to externally quantify painful regions using electrodermal properties[14] and superficial soft tissue stiffness measurements.[15] Although both electrical resistance and tissue stiffness significantly changed at areas where myofascial trigger points existed, neither was able to distinguish between tissue properties of active and latent trigger points. Electromyography has also been used to measure end plate noise at myofascial trigger points before and after treatment with an acupuncture needle.[16] Electromyography has shown that end plate noise at trigger point sites decreased as pain decreased after acupuncture treatment. However, only active trigger points had a local twitch response during needling.[16] Human in vivo microdialysis studies of the upper trapezius muscle have found that active sites have a unique biochemical milieu compared to latent sites and palpably normal muscle. Active sites have a more acidic milieu and higher levels of inflammatory mediators, neuropeptides, catecholamines, and cytokines—substances known to be associated with persistent pain states, inflammation, and sensitization.[9,10]

Other noninvasive methods are currently being explored to visualize and characterize myofascial trigger points via magnetic resonance elastography.[17] Magnetic resonance elastography is attractive because magnetic

resonance imaging is the diagnostic standard for musculoskeletal imaging; however, it is an expensive and less accessible method compared to other imaging modalities such as sonography. Sonography is a readily available, portable, and inexpensive imaging modality, suitable for use in a physiatrist's office to complement physical examination, guide therapeutic interventions, and evaluate treatment outcomes. Previously, our group showed the feasibility of sonography for visualizing trigger points and the surrounding soft tissue.12 We were able to visualize trigger points and score them on an ordinal scale using gray scale B-mode images, color variance elastography, and Doppler waveforms of local blood flow from 9 patients. The goal of this study was to expand on these preliminary findings to study a larger set of patients and develop quantitative measures of the soft tissue environment of myofascial trigger points. We hypothesize that the soft tissue environments of active trigger points, latent trigger points, and normal muscle differ as measured by sonoelastography and Doppler imaging. We also wanted to explore the sensitivity of these measures to change after a common treatment, dry-needling therapy, to evaluate the feasibility of this method for monitoring posttreatment clinical outcomes.

Materials and Methods

Study Population and Clinical Examination

This study was conducted at the Rehabilitation Medicine Department of the National Institutes of Health Clinical Research Center. Forty-four patients with acute cervical pain met inclusion criteria, having either an active or a latent myofascial trigger point in one or both upper trapezii, and underwent a thorough musculoskeletal evaluation to rule out potential causes of their symptoms other than myofascial trigger points. Patients were classified as having active trigger points if they had pain consistently over the past 3 months or as having latent trigger points or normal muscle if they had no pain over the past 3 months. Patients with posttraumatic pain were also included in the study unless they met the exclusion criteria listed previously, which included fibromyalgia, atypical facial neuralgia, myopathy, radiculopathy, history of shoulder or spine surgery, and trigger point injections.12 The Institutional Review Board of the National Institute of Dental and Craniofacial Research approved this study, and each participant provided informed consent to participate in the study.

The patients underwent a physical examination as previously described.12 Briefly, the presence or absence of myofascial trigger points in the upper trapezius muscle was determined by the criteria of Simon et al18 according to standard clinical practice. Palpation was in the central region of the upper trapezius muscle within 6 cm of the muscle's midline (approximately midway between the cervical vertebrae and the acromion process. The examination resulted in marking of 4 sites, 2 on each side (ie, the right and left trapezius). Sites were considered normal if no palpable nodule was found. Active sites had at least 1 palpable nodule, and palpation reproduced or exacerbated the patient's spontaneous pain, thereby classifying the site as active. Latent sites had 1 or more palpable nodules; although tender to palpation, this maneuver did not reproduce or exacerbate the patient's spontaneous pain. The sites being analyzed were at least 5 cm apart from one another. Patients were asked to rate the level of pain on each side of their neck using a visual analog scale to ranging from 0 to 10 (0, least painful; 10, most painful). A pressure algometer (Pain Diagnostics and Treatment, Great Neck, NY) was used on each of the 4 sites to determine the pain pressure threshold, defined as the amount of pressure needed to produce pain. Only the examiner knew the clinical status of the patients (ie, whether they had cervical pain) and classifications of the marked sites. The sonographers were blinded to the clinical status when acquiring sonographic data. Approximately 30 minutes elapsed between the algometric procedures and sonography, and all of the test procedures were completed in less than 2 hours.

Imaging

Each participant underwent a sonographic examination using an iU22 clinical ultrasound system (Philips Health-care, Bothell, WA) with a 12–5-MHz linear array L12-5 transducer as previously described.12 Briefly, the 4 marked sites were targeted to determine whether myofascial trigger points could be visualized in the upper trapezius. Typically, trigger points appear as focal hypoechoic (darker) areas with a heterogeneous echo texture.

To determine the area of these stiffer zones of muscle tissue vibration, sonoelastography was performed using an external vibration source of approximately 92 Hz. As described previously,[12,19] a handheld vibrating massager (Mini Vibrator; North Coast Medical, Inc, Morgan Hill, CA) was applied 2 to 3 cm from each site to be imaged. The color variance mode was used to image wave propagation through the myofascial trigger points of vibrations induced by the massager (Figure 1).

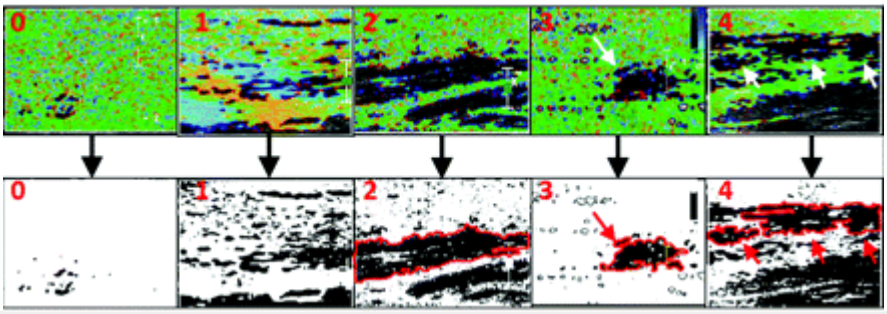

Figure 1. Color Doppler images (top row) of the vibrating trapezius muscle and binary images (bottom row) for trigger point area calculation of stiffer tissue zones. Muscle tissue was scored as follows: 0, uniform echogenicity and stiffness; 1, noisy image, no clear nodule; 2, taut band; 3, focal stiff nodule; and 4, multiple nodules. Arrows denote focal trigger points, and red outlined areas denote measured trigger point areas.

The vasculature around marked sites was assessed with color Doppler imaging, and the flow velocity waveforms were measured with spectral Doppler imaging. Flow waveforms in blood vessels with pulsatile flow (arteries or enlarged arterioles, typically >1 mm in diameter) that were found within 1 to 2 cm of palpable trigger points were analyzed to calculate the resistivity index [RI; (peak systolic velocity – minimum diastolic velocity)/peak systolic velocity] and pulsatility index [PI; (peak systolic velocity – minimum diastolic velocity)/mean velocity]. In normal muscle, the RI is 1, indicating no diastolic flow. Elevated diastolic flow (RI <1) indicates decreased vascular resistance, and negative diastolic flow (RI >1) indicates increased vasculature bed resistance. Both the RI and PI are common measures used to determine the volumetric blood flow in muscle tissue[20] and the lower extremities[21] on Doppler sonography.

Image Analysis

In a previous study, our group devised 2 ordinal scores to describe tissue and blood flow characteristics of the imaged sites.[12,19] Tissue imaging scores ranged from 0 (normal, uniform echogenicity and stiffness) to 4 (abnormal structure with multiple focal hypoechoic and stiff nodules; Figure 1). The blood flow waveform score (from the Doppler flow waveform) ranged from 0 (normal arterial flow) to 2 (abnormal high-resistance flow with retrograde diastolic flow; Figure 2). In this study, more quantitative measurements were performed from the elastographic and Doppler flow waveform images using ImageJ.[22,23]

Elastographic color variance images were imported into ImageJ, where they were scaled and cropped for the area of interest. Trigger point areas were then calculated similarly to automated cell-counting methods.[23] Briefly, the image was converted to binary; the dark areas were automatically selected; and the area was calculated on the basis of scaling (Figure 1).

Doppler flow waveform images were analyzed similarly to elastographic images. Blood flow waveforms were imported into ImageJ, scaled, and cropped for the waveform of interest. The peak systolic velocity and minimum diastolic velocity were measured. The time-averaged mean velocity was calculated by integrating the area under the velocity waveform for the entire cardiac cycle and dividing by the duration of the cardiac cycle (Figure 2).

Statistical Analysis

Statistical analysis was done with PASW 18 software (SPSS Inc, Chicago, IL) using 1-way analysis of variance and the Tukey post hoc test for normally distributed data. Normal data are presented as mean ± SD. Non-normally distributed data were analyzed via Kruskal-Wallis 1-way analysis of variance and the Dunn test for post hoc comparison. Statistical significance was determined at $P < .05$. Receiver operating characteristic

(ROC) curves were generated to measure the binary classification strength of the different objective measures in this study.

Previous SectionNext Section

Results

The age range of the 44 patients was 22 to 57 years. A total of 169 sites were imaged via sonography, of which 84 were located medially in the upper trapezius, and 85 were located laterally. In some patients, not all of the 4 clinically identified sites could be imaged on sonography because of scheduling restrictions. Active and latent trigger points were more often located medially (37 of 49 total sites) than laterally (39 of 52 sites). Only 9 of the 68 normal sites were located medially. Approximately 83% of the active sites had a symmetric active or latent site located on the bilateral trapezius muscle.

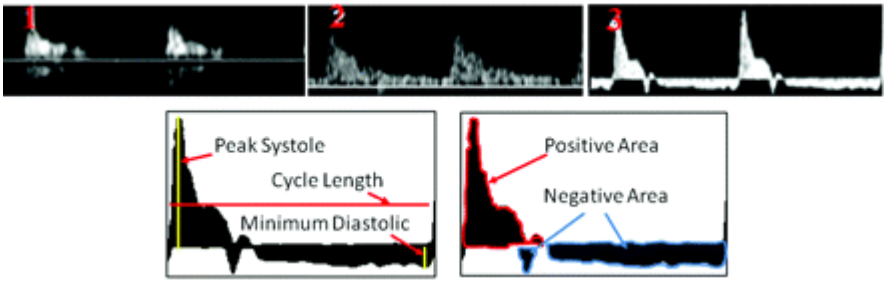

Figure 2. Color Doppler waveform images (top tow) of blood flow through the trapezius muscle and binary images (bottom row) for pulsatility and resistivity index calculations. Waveforms were scored as follows: 1, high-resistance flow with no diastolic flow; 2, elevated diastolic flow; and 3, sustained retrograde flow in diastole.

Active and latent sites had significantly lower pain pressure thresholds than normal sites ($P < .05$) and active sites had lower pain pressure thresholds than latent sites ($P < .05$; Figure 3). Receiver operating characteristic curves were generated to evaluate the binary classification strength of pain pressure threshold scores to be able to delineate normal sites from active or latent sites and active from latent sites (Figure 4). The ROC curves determined pain pressure threshold scores to be fair classifiers of active versus normal sites (cutoff point, 4.07; area under the curve [AUC], 0.72; $P < .01$) and poor classifiers of latent versus normal sites (cutoff point, 4.07; AUC, 0.64; $P < .05$) but failed to classify active versus latent sites (cutoff point, not applicable; AUC, 0.55).

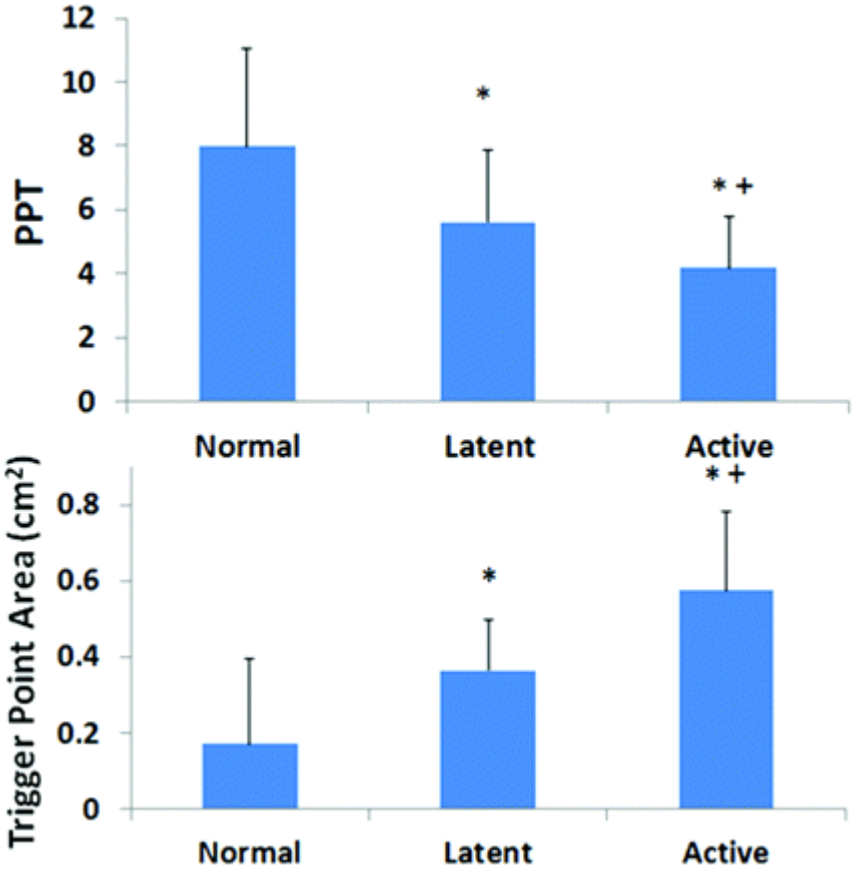

Figure 3. Plots of pain pressure threshold (PPT) scores and trigger point areas. *Significant difference from normal sites; [+]significant difference from latent sites ($P < .05$).

Trigger point areas assessed by vibration elastography showed trends similar to those of pain pressure threshold scores (Figure 3). Active and latent sites had significantly higher areas compared to normal sites ($P < .01$), and active sites were significantly larger than latent sites ($P < .01$). The ROC curves showed that trigger point area measurements were excellent classifiers of active versus normal sites (cutoff point, 0.35; AUC, 0.9; $P < .01$), fair classifiers of latent versus normal sites (cutoff point, 0.27; AUC, 0.79; $P < .01$), and fair classifiers of active versus latent sites (cutoff point, 0.4; AUC, 0.8; $P < .01$). The pain pressure threshold was not linearly correlated to the trigger point area, even though similar trends were observed across latent and active sites (data not shown).

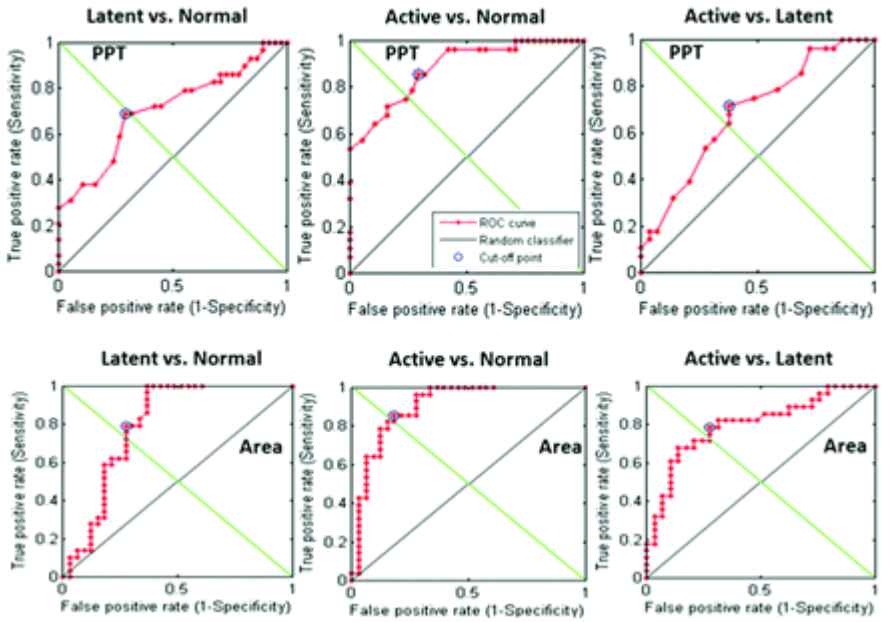

Figure 4. Receiver operating characteristic curves for pain pressure threshold (PPT) scores (top row) and trigger point areas (bottom row) comparing the classification strength between latent and normal, active and normal, and active and latent sites. Red lines indicate receiver operating characteristic curves; black diagonals, random classifiers; and circles, cutoff points for a successful test.

On color Doppler imaging, prominent blood vessels were observed in the close vicinity of trigger points. In 27 of the 49 active sites (55%), retrograde diastolic flow was observed compared to 21 (40%) and 15 (31%) for latent and normal sites, respectively. The occurrence of retrograde flow was significantly higher in active and latent sites compared to normal tissue ($P < .01$). The PI values were significantly different in active compared to normal sites ($P < .05$; Figure 5). No differences in RI values were detected between normal (Figure 5), latent, and active sites. Using ROC analysis, it was found that the PI was not a good classifier of active, latent, or normal sites because of the large variance.

A 3-dimensional scatterplot of the visual analog scale versus the pain pressure threshold versus the area (Figure 6) showed that the visual analog scale and trigger point area separated latent and active groups well, but the pain pressure threshold did not. This finding was similar to what was shown from the ROC curves. Plotting the PI versus the visual analog scale versus the area further separated active and latent groups while also showing the increased PI variance in active trigger points.

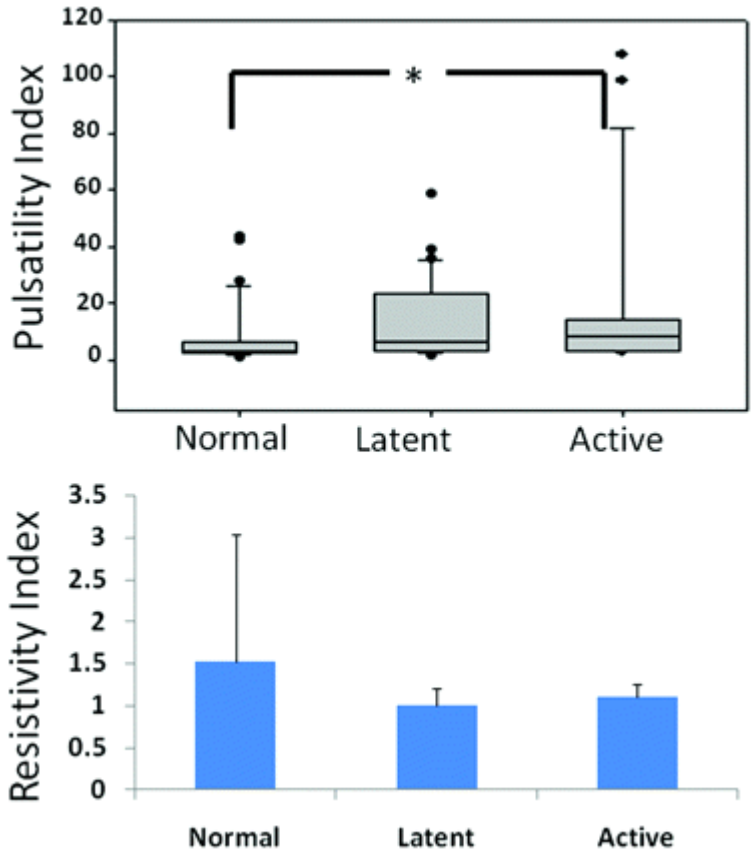

Figure 5. Plots of the pulsatility and resistivity indices for normal, latent, and active sites. *Significant difference ($P < .05$).

Discussion

This study investigated quantitative methods for characterizing the soft tissue environment of active and latent myofascial trigger points compared to palpably normal muscle using sonographic techniques. We found that vibration elastography was an effective method for measuring the trigger point size and was excellent for distinguishing the site type (normal, latent, or active). Sonographic techniques can play in a role in objectively identifying active and latent myofascial trigger points, developing outcome measures after therapeutic intervention, and better describing the complex environment surrounding myofascial trigger points.

Active and latent trigger points have 3 clinical attributes that separate them from normal tissue and must be investigated to explain the pathogenesis and pathophysiologic mechanisms of myofascial pain syndrome. Additional attributes, which further distinguish active from latent points, may also warrant further investigation. One attribute is the change in muscle mechanical characteristics indicated by a hard palpable nodule within a taut band of contractured muscle. Another attribute is the presence of local or referred tenderness and the presence of spontaneous or induced pain. The pain can be localized to the palpable nodule, referred to a satellite location, or both.4 The third attribute is an increased presence of highly resistive vascular beds at or near latent and active trigger points.

As such, it would seem logical that as the trigger point area increased there would have been an associated increase in pain sensitivity (ie, a lower pain pressure threshold score). In our study, we did not find a correlation between trigger point areas and pain pressure threshold scores for either latent or active sites (Figure 3). This finding implies that although active sites have larger trigger point areas and lower pain pressure threshold scores (more tender, ie, pain elicited with less pressure) than latent sites, size and pain pressure threshold scores are not directly linked. As a result, the data suggest that other mechanisms could be contributing independently to the trigger point size and pain sensitivity. In fact, the pain pressure threshold may depend on the presence of sensitizing biochemicals such as neuropeptides and catecholamines and only

secondarily on mechanical properties.[10] It is believed that the stiffer hypoechoic nodules are a result of increased muscle fiber contraction and recruitment or local injury that can also cause regions of ischemia.[24]

The pathogenesis of myofascial trigger points is not completely understood. One hypothesis is that trigger points form as a result of muscle overload. For example, patients commonly report an onset of pain associated with myofascial trigger points after acute, repetitive, prolonged, or chronic muscle overload. Piano students developed significantly decreased pressure thresholds over latent myofascial trigger points after only 20 minutes of continuous piano playing.[17] Computer operators developed myofascial trigger points after as little as 30 minutes of continuous typing.[25] These data suggest that even low-level muscle contractions accompanying stereotypical movement patterns can contribute to the development of myofascial trigger points and have been shown to lead to muscle fiber degeneration, an increase in Ca^{2+} release, energy depletion, and the release of various cytokines, which all have been associated with the formation of trigger points.[26–28] During low-level contractions, the intramuscular pressure increases considerably, especially near the muscle insertions, which may impair the local circulation, cause hypoxia, and eventually lead to trigger point formation.[24,29–31] Measures that link the change in fiber structure, localized tissue stiffness, and blood flow properties to the biochemical milieu of myofascial trigger points could help elucidate the mechanobiological relationships in normal muscle and muscle affected by trigger points. Other biochemical information (eg, substances associated with muscle metabolism) is still needed to provide an adequate framework in which biochemistry is linked to the mechanical environment of the muscle. Although the cascade of changes in the muscle that lead to myofascial trigger points has not been fully mapped, the biochemical environment of the active trigger point has been found to be more acidic and to have elevated levels of inflammatory mediators, neuropeptides, and proinflammatory cytokines that are typically associated with persistent pain and tenderness (as indicated by the pain pressure threshold scores).[9,10]

The integrated trigger point hypothesis proposes capillary constriction and increased metabolic demands as factors contributing to the development of myofascial trigger points. Therefore, ischemia and hypoxia may result at the site of the trigger point, sensitizing peripheral and central nociceptors and causing more pain and tenderness.[31] Increased hypoxia in muscle tissue is usually followed by increased levels of angiogenic factors and blood vessel formation, which we observed in both active and latent sites. Blood vessel formation or expansion may result from vascular endothelial growth factor, chemokines, and chemotactic agents (tumor necrosis factor α and transforming growth factor β), which can be stimulated by factors other than ischemia.[32–35]

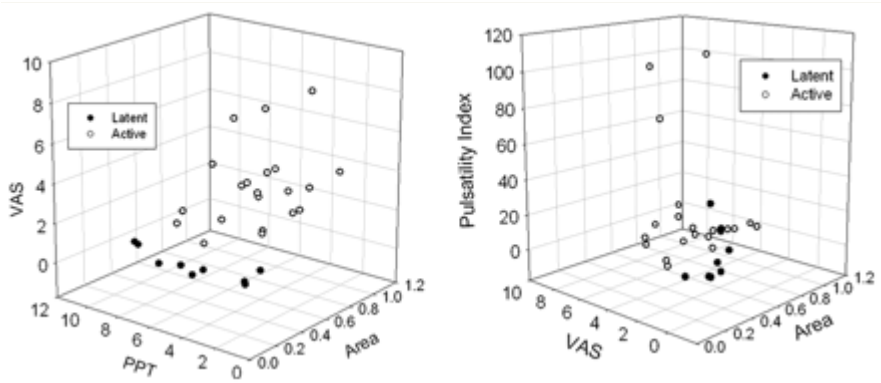

Figure 6. Three-dimensional plots of the visual analog scale (VAS) versus the pain pressure threshold (PPT) versus the trigger point area (left) and the pulsatility index versus the visual analog scale versus the area (right) for patients with latent and active sites. The visual analog scale and trigger point area measures separate latent and active data the most, whereas the pulsatility index shows the largest amount of variance in patients with active sites.

In this study, results from the Doppler waveforms of blood flow showed significantly different blood flow characteristics in active sites compared to normal tissue (Figure 5). The arteries in the neighborhood of active and latent sites had highly pulsatile blood flow with retrograde diastolic flow more often than normal tissue. Two factors could explain highly pulsatile blood flow. The first is an increase in the compliance and volume of the vascular compartment, and the second is an increase in outflow resistance. The importance of altered retrograde blood in the context of variable pain characteristics (eg, its presence or absence, intensity, location, and referral) and the tenderness associated with active versus latent myofascial trigger points is yet to be fully

understood. However, the increased presence of blood vessels could provide some intriguing clues to the pathophysiologic mechanisms underlying the development of myofascial trigger points and the natural history of myofascial pain syndrome. Increased outflow resistance could be due to muscle contracture at the trigger point that compresses the capillary/venous bed, anatomic factors related to the geometry of the apex of the upper trapezius muscle that apply external compressive pressure, local vasoconstriction due to inflammation, or externally applied pressure from the ultrasound transducer during imaging.

Although a significant difference was found between active and normal sites for the PI, the RI values were very similar across all sites (Figure 5). We suspect the large variance in the PI and similar RI values between sites was due to the proximity normal sites had to latent and active trigger points and vice versa. Because all of the patients in this study had at least 1 palpable trigger point, the blood flow characteristics we observed in the upper trapezius do not represent the normal variation. The impaired muscle tissue could result in abnormal blood flow characteristics in normal sites. However, monitoring blood flow characteristics could still prove useful for monitoring areas around trigger points and how they may change over time or after treatment.

Data for a pilot study including 3 active cases and 1 latent case were gathered at different time points (Figure 7) to observe the behavior of trigger points after dry needling treatment. The visual analog scale for 2 of the 3 active cases decreased with time, whereas the latent case remained constant. The pain pressure threshold scores increased for all active cases, whereas the latent group remained constant. The trigger point area and PI decreased for all 3 active cases with time but increased slightly for the latent case. For these few cases treated with dry needling, we did observe fairly consistent changes and improvements regarding the size and blood flow of active sites in the trapezius (Figure 7). The latent site did not show any changes, but the changes in the active sites agree with other work showing decreased end plate noise at active sites.16 Although there were too few follow-up cases to draw conclusions, the data do show promise that these measures can be used to follow patient responses to treatment.

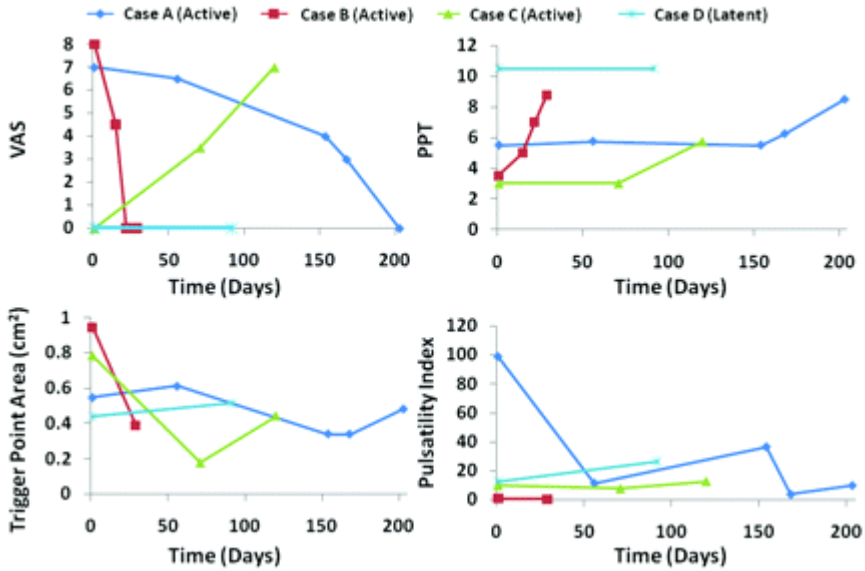

Figure 7. Follow-up data plots of the visual analog scale (VAS), pain pressure threshold (PPT), trigger point area, and pulsatility index versus time. Data are from 3 patients with active sites and 1 patient with latent sites that underwent dry needling after the initial visit and sonographic examination.

We used 3-dimensional plots to analyze data to detect interactions that would separate latent and active sites (Figure 6). The data plotted included active site data for patients with active sites (thus excluding all normal and latent site data for that patient) and only latent site data for patients not having any active sites (thus excluding normal site data). This analysis was done for 2 reasons: First, it was suspected that latent sites in patients with active sites might not be true latent trigger points. In other words, latent sites in patients with active sites could provide confounding information because of the pain elicited by neighboring active sites. Second, visual analog scale data were reported for the left and right sides, not by site. Thus, the visual analog scale score would be attributed to the most symptomatic site (ie, active over latent or latent over normal). The 3-dimensional plots show that the visual analog scale and trigger point area separated latent from active sites

most successfully, as confirmed by the ROC curves. It is not surprising that the visual analog scale score would have such a large impact on grouping data because it is one of the main scores clinicians use to screen for myofascial trigger points.

Although most trigger points are located and classified on the basis of the patient's history and a physical examination, results can vary depending on the clinician's training and experience. We sought to develop methods to locate and quantitatively assess myofascial trigger points that can aid in classifying tissue types and monitoring changes over time. The visual analog scale, pain pressure threshold scores, and palpation are the reference standards for detecting and classifying trigger points, but they are still subjective measures.36 Pain pressure threshold scores are more objective and serve as fair measures for distinguishing normal sites from trigger point sites, but pain pressure threshold scores still have the perception of what each patient determines the pain threshold to be.36 Blood flow measures from current symptomatic patients did not perform well as classifiers of the site type because of the large variance. The role of blood flow and the presence of enlarged blood vessels in or around trigger points has not been studied. The trigger point area proved to be a very good classifier of the site type in the upper trapezius and was also quick and simple to implement using a clinical sonographic system (Figure 4).

Although we believe that measuring the trigger point area and PI at symptomatic sites can aid in distinguishing between active, latent, and normal sites, there were some limitations to this study. First, our study did not include a control group of pain-free patients. Instead, pain-free sites were marked at least 5 cm apart from latent and active sites. Site locations were standardized as mentioned in "Materials and Methods" in an attempt to measure the symmetry of site locations. Second, no biochemical analysis was conducted to link biochemical markers to differences in trigger point sizes and blood flow properties. Therefore, universal generalization to myofascial pain syndrome and myofascial trigger points is premature, as is development of a definitive model to explain the etiology of myofascial trigger points. Last, the vibrating massager used in this study was an off-the-shelf handheld device with only a single vibrating frequency. Acquiring trigger point area measurements at different frequencies would confirm that area measurements are frequency independent and furthermore would provide data necessary to measure shear elasticity.

Future work needs to focus on linking the physical properties measured here and the biochemical changes in the muscle tissue. More data on the mechanical properties of trigger points need to be obtained. The heterogeneity of the fiber structure and the compressive or shear moduli of these areas may provide important clues to the pathogenesis or pathophysiologic mechanisms of myofascial trigger points. Last, tracking the changes in mechanical properties and the muscle fiber structure along with the biochemical milieu in trigger points after treatment may provide a better understanding of the physiologic environment in the muscle tissue.

The approach presented here provides a quick and effective method for quantitatively classifying myofascial trigger points in the upper trapezius. Measuring the trigger point area could serve as an acceptable outcome measure for assessing different treatments.

References

1. Fishbain DA, Goldberg M, Meagher BR, Steele R, Rosomoff H.. *Male and female chronic pain patients categorized by DSM-III psychiatric diagnostic criteria. Pain 1986; 26:181–197.*
2. Kao MJ, Han TI, Kuan TS, Hsieh YL, Su BH, Hong CZ. *Myofascial trigger points in early life. Arch Phys Med Rehabil 2007; 88:251–254.*
   Medline
3. Borg-Stein J, Simons DG. *Focused review: myofascial pain. Arch Phys Med Rehabil 2002; 83:S40–S49.*
   Medline
4. Alvarez DJ, Rockwell PG. *Trigger points: diagnosis and management. Am Fam Physician 2002; 65:653–660.*
   Medline
5. Lucas KR. *The impact of latent trigger points on regional muscle function. Curr Pain Headache Rep 2008; 12:344–349.*
   Medline

6. Fernández-de-Las-Peñas C, Simons D, Cuadrado ML, Pareja J. *The role of myofascial trigger points in musculoskeletal pain syndromes of the head and neck. Curr Pain Headache Rep 2007; 11:365–372.*
CrossRefMedline

7. Windisch A, Reitinger A, Traxler H, et al. *Morphology and histochemistry of myogelosis. Clin Anat 1999; 12:266–271.*
CrossRefMedline

8. Mense S. *The pathogenesis of muscle pain. Curr Pain Headache Rep2003; 7:419–425.*
CrossRefMedline

9. Shah JP, Phillips TM, Danoff JV, Gerber LH. *An in vivo microanalytical technique for measuring the local biochemical milieu of human skeletal muscle. J Appl Physiol 2005; 99:1977–1984.*
Abstract/FREE Full Text

10. Shah JP, Danoff JV, Desai MJ, et al. *Biochemicals associated with pain and inflammation are elevated in sites near to and remote from active myofascial trigger points. Arch Phys Med Rehabil 2008; 89:16–23.*
CrossRefMedline

11. Kuan TS, Hong CZ, Chen JT, Chen SM, Chien CH. *The spinal cord connections of the myofascial trigger spots. Eur J Pain2007; 11:624–634.*
Medline

12. Sikdar S, Shah JP, Gebreab T, et al. *Novel applications of ultrasound technology to visualize and characterize myofascial trigger points and surrounding soft tissue. Arch Phys Med Rehabil 2009; 90:1829–1838.*
CrossRefMedline

13. Niddam DM, Chan RC, Lee SH, Yeh TC, Hsieh JC. *Central modulation of pain evoked from myofascial trigger point. Clin J Pain 2007; 23:440–448.*
Medline

14. Shultz SP, Driban JB, Swanik CB. *The evaluation of electrodermal properties in the identification of myofascial trigger points. Arch Phys Med Rehabil 2007; 88:780–784.*
CrossRefMedline

15. Arokoski JP, Surakka J, Ojala T, Kolari P, Jurvelin JS. *Feasibility of the use of a novel soft tissue stiffness meter. Physiol Meas 2005; 26:215–228.*
Medline

16. Chou LW, Hsieh YL, Kao MJ, Hong CZ. *Remote influences of acupuncture on the pain intensity and the amplitude changes of endplate noise in the myofascial trigger point of the upper trapezius muscle. Arch Phys Med Rehabil 2009; 90:905–912.*
Medline

17. Chen Q, Basford J, An KN. *Ability of magnetic resonance elastography to assess taut bands. Clin Biomech (Bristol, Avon) 2008; 23:623–629.*
Medline

18. Simons DG, Travell JG, Simons LS. *Myofascial Pain and Dysfunction: The Trigger Point Manual. 2nd ed. Baltimore, MD: Williams & Wilkins; 1999.*

19. Sikdar S, Shah JP, Gilliams E, Gebreab T, Gerber LH . *Assessment of myofascial trigger points (MTrPs): a new application of ultrasound imaging and vibration sonoelastography. Conf Proc IEEE Eng Med Biol Soc 2008; 2008:5585–5588.*
Medline

20. Ariji Y, Kimura Y, Gotoh M, Sakuma S, Zhao YP, Ariji E. *Blood flow in and around the masseter muscle: normal and pathologic features demonstrated by color Doppler sonography. Oral Surg Oral Med Oral Pathol Oral Radiol Endod 2001; 91:472–482.*
CrossRefMedline

21. Holland CK, Brown JM, Scoutt LM, Taylor KJ. *Lower extremity volumetric arterial blood flow in normal subjects. Ultrasound Med Biol 1998; 24:1079–1086.*

22. Abramoff MD, Magalhães P, Ram SJ. *Image processing with ImageJ. Biophotonics Int 2004; 11:36–42.*

23. van der Laak JA, Schijf CP, Kerstens HM, Heijnen-Wijnen TH, de Wilde PC, Hanselaar GJ. *Development and validation of a computerized cytomorphometric method to assess the maturation of vaginal epithelial cells. Cytometry 1999; 35:196–202.*CrossRefMedline

24. Jarvholm U, Styf J, Suurkula M, Herberts P. *Intramuscular pressure and muscle blood flow in supraspinatus. Eur J Appl Physiol Occup Physiol 1988; 58:219–224.*Medline

25. Treaster D, Marras WS, Burr D, Sheedy JE, Hart D. *Myofascial trigger point development from visual and postural stressors during computer work. J Electromyogr Kinesiol 2006; 16:115–124.*Medline

26. Febbraio MA, Pedersen BK. *Contraction-induced myokine production and release: is skeletal muscle an endocrine organ? Exerc Sport Sci Rev 2005; 33:114–119.* CrossRefMedline

27. Gissel H. *Ca^{2+} accumulation and cell damage in skeletal muscle during low-frequency stimulation. Eur J Appl Physiol 2000; 83:175–180.*CrossRefMedline

28. Lexell J. *Ageing and human muscle: observations from Sweden. Can J Appl Physiol 1993; 18:2–18.*Medline

29. Otten E. *Concepts and models of functional architecture in skeletal muscle. Exerc Sport Sci Rev 1988; 16:89–137.*Medline

30. Simons DG. *Review of enigmatic MTrPs as a common cause of enigmatic musculoskeletal pain and dysfunction. J Electromyogr Kinesiol 2004; 14:95–107.* CrossRefMedline

31. Gerwin RD, Dommerholt J, Shah JP. *An expansion of Simons' integrated hypothesis of trigger point formation. Curr Pain Headache Rep 2004; 8:468–475.*
CrossRefMedline

32. Beck L Jr., D'Amore PA. *Vascular development: cellular and molecular regulation. FASEB J 1997; 11:365–373.*
Abstract

33. Benjamin LE, Hemo I, Keshet E. *A plasticity window for blood vessel remodelling is defined by pericyte coverage of the preformed endothelial network and is regulated by PDGF-B and VEGF. Development 1998; 125:1591–1598.*
Abstract

34. Lloyd RV, Vidal S, Horvath E, Kovacs K, Scheithauer B. *Angiogenesis in normal and neoplastic pituitary tissues. Microsc Res Tech 2003; 60:244–250.*
CrossRefMedline

35. Voronov E, Carmi Y, Apte RN. *Role of IL-1-mediated inflammation in tumor angiogenesis. Adv Exp Med Biol 2007; 601:265–270.*
Medline

36. Prushansky T, Handelzalts S, Pevzner E. *Reproducibility of pressure pain threshold and visual analog scale findings in chronic whiplash patients. Clin J Pain 2007; 23:339–345.*
Medline

O autor cita como limitações da Elastografia músculo esquelética:

- É muito operador dependente;
- Se houver pressão excessiva da sonda sobre o tecido examinado altera-se a consistência artificialmente e o resultado estará destorcido;
- Anisotropia é evidente em muitos casos e tem que ser corrigida pelo operador;
- Variabilidade inter e intra observador.

Conclusão: é uma técnica promissora e de grande potencial, mas ainda está nos primórdios do seu desenvolvimento, principalmente na área do músculo esquelético.

A terceira palestra foi sobre **INJEÇÃO DE ESTERÓIDE NO OMBRO: PROCEDIMENTO ÀS CEGAS VS DIRECIONADO PELO US**, ministrada por David Fessel, da Universidade de Michigan.

As injeções de esteróides nas articulações iniciaram em 1950 mas houve muitas complicações decorrentes do procedimento, principalmente a necrose local da pele, dispigmentação da pele (4%), infecção local e ruptura do tendão. Esta última complicação que é muito ruim se ocorrer, decorre quando a injeção é realizada intra tendão, pois ela induz a necrose do tendão e, como a dor desaparece e o paciente se sente bem, ele abusa da força e rompe o tendão. Ele relata o caso de um jogador de baseball muito famoso que teve essa complicação após o procedimento e mostrou a foto do atleta durante o episódio de ruptura em um jogo que participou (o último, pois não teve mais condição física após isso). Portanto, para que se realize as injeções de esteróide é necessário o correto posicionamento da agulha. Se a injeção for às cegas, nunca se sabe exatamente onde está sendo aplicada a injeção: gordura? Músculo? Bursa? Junta? Tendão? A injeção músculo esquelética às cegas é muito imprecisa, pois 29% dos casos ela é aplicada intra tendão. Portanto, as injeções realizadas corretamente fazem toda a diferença e há melhora significante dos sintomas em relação às injeções às cegas. O risco de ruptura do tendão reduz significantemente se a injeção for guiada por US. Mostrou vários exemplos:

1. Caso de Fluido injetado intra bursa subdeltóide
2. Caso de Atrofia crônica e ruptura
3. Caso de ruptura completa do tendão após múltiplas injeções
4. Caso de ruptura parcial
5. Casos pós cirúrgicos.

Mencionou dois artigos de referência:

Using Sonography to Reveal and Aspirate Joint Effusions

1. **D. P. Fessell[1], J. A. Jacobson[1], J. Craig[2], G. Habra[2], A. Prasad[2], A. Radliff[2] and M. T. van Holsbeeck[2]**

Traditionally, joint aspiration has been performed using only external anatomic landmarks (“blind” aspiration) or fluoroscopic guidance. We illustrate the technique and role of joint aspiration of the shoulder, elbow, hip, knee, and ankle with sonographic guidance. Sonographic evaluation and guidance of aspiration offers several advantages over the traditional approaches. The joint can first be examined to determine if fluid is present. This examination can eliminate a potentially traumatic and unnecessary aspiration attempt of a joint that does not contain an effusion.

In addition to joint effusions, sonography can reveal fluid collections, such as bursitis and soft-tissue abscesses, outside the joint. Many soft-tissue abscesses and distended bursae can be detected on physical examination. Not infrequently, however, there is a clinical question of an abscess in a patient with cellulitis, soft-tissue edema, or obesity that limits the physical examination. In such patients, there may also be a question of a joint effusion. Sonographic examination allows detection of joint fluid as well as soft-tissue fluid collections and avoids contamination of an aseptic joint that could occur by blind or fluoroscopic aspiration through an overlying soft-tissue infection such as an abscess, septic bursitis, or septic tenosynovitis.

Technique

For each joint, the aspiration approach is similar to that used for arthrography, but the approach is guided by the location of fluid detected sonographically. A commercial arthrogram tray and a 20-gauge spinal needle with stylet are commonly used for aspiration. Sonography of the joint in at least two planes is first performed to precisely localize the effusion [1]. A linear transducer of at least 7.5 MHz is recommended for all joints except the hip, where a curvilinear 5-MHz or lower frequency transducer may be required, depending on the patient's body habitus. The appearance of an effusion (complex, hypoechoic, anechoic) does not predict an inflammatory or infectious cause [2]. If a suspected fluid collection contains a region that is anechoic in

addition to regions that are hypoechoic or echogenic, we usually have success in aspirating fluid from the more anechoic region.

Doppler evaluation is routinely used to assess for vascular structures surrounding the effusion or along the potential aspiration approach. Increased power Doppler flow around a fluid collection can be shown in some effusions with an infectious or inflammatory cause; however, lack of increased flow on power Doppler imaging does not exclude infection [3]. Doppler flow within a hypoechoic collection surrounding a joint suggests synovitis or other soft-tissue process and is not compatible with a simple joint effusion [4].

If a joint effusion is detected, the depth from the skin surface to the deepest portion of the fluid is measured along the proposed needle tract. A needle with an appropriate length is selected. With the transducer positioned over the effusion, an ink dot is placed on the skin at the midpoint of each side of the transducer. The dots are connected to form a "+". Accuracy of the marking is checked by placing the transducer at the "+" in both transverse and longitudinal orientations. An inaccurate skin marking is one potential cause of an unsuccessful aspiration; care must taken to ensure the marking is directly over the center of the effusion. We routinely perform aspiration using a freehand technique. However, a guide can be installed on the transducer to direct the needle if desired [1].

For large and easily accessible effusions, sonography can simply be used for detection, marking of the effusion, and exclusion of a soft-tissue process such as an abscess. In such cases, sonographic guidance during needle placement is not required. If there are no contraindications, the skin is cleansed with Clinidine (povidoneiodine; Clinipad, Rocky Hill, CT) and anesthetized with 1% lidocaine. The bevel of the needle is positioned adjacent to the rounded portion of the joint (e.g., the bevel is toward the humeral head during shoulder aspiration). After sonographic evaluation, if aspiration without sonographic guidance is selected, the needle should be advanced as parallel as possible to the axis of the ultrasound waves. Advancement of the needle with excessive angulation from this axis is a potential pitfall. Ideally, a straight horizontal axis (as with posterior shoulder aspiration performed with the patient in the sitting position) or a straight vertical axis (as with hip aspiration in the supine position) is used. The needle is advanced to the level of the osseous structures and suction from the syringe is applied.

If no fluid is noted after suction is applied, the needle can be rotated clockwise or counterclockwise to adjust the bevel. The stylet can also be replaced and moved to and fro within the needle to dislodge any debris in the needle. The needle is withdrawn slowly, a millimeter at a time, with continuous suction from the syringe.

If the initial aspiration attempt is unsuccessful, the skin marking can be rechecked with sonography, or sonographic guidance during needle positioning can be used. For small or less accessible effusions, sonographic guidance of needle placement is used with the initial aspiration. A sterile cover is placed over the transducer and sterile gel applied. A compact linear or "hockey stick" probe (Fig. 1A,1B,1C) facilitates scanning during aspiration.

Fig. 1A. —Glenohumeral joint aspiration using sonographic guidance. Photograph shows transducer positioning for transverse sonography of posterior right shoulder and needle positioning for aspiration. For purposes of illustration, a sterile transducer cover and drape are not shown.
are not shown.

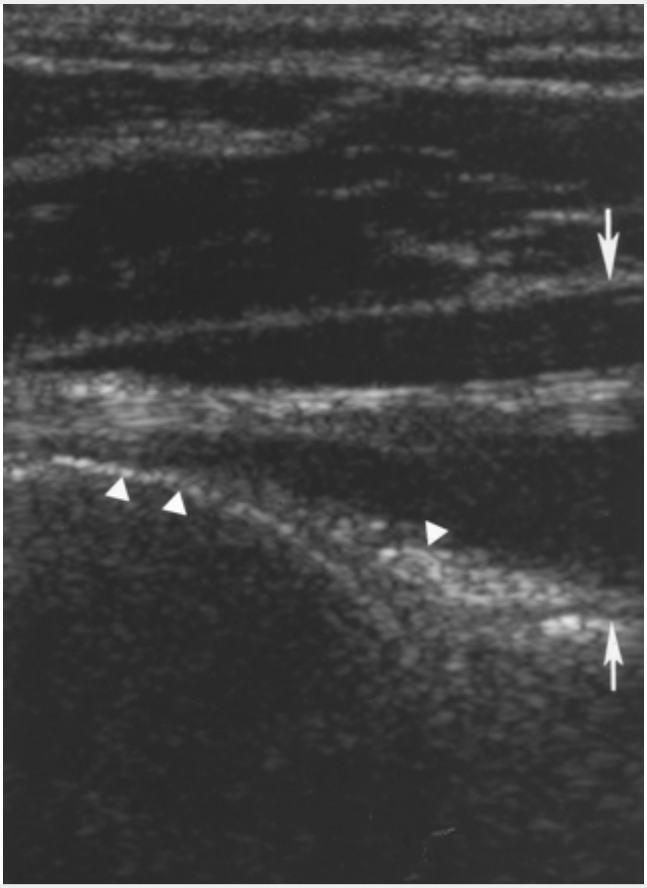

Fig. 1B. —Glenohumeral joint aspiration using sonographic guidance. Transverse sonogram of normal posterior glenohumeral joint, scanned as illustrated in **A**, shows no detectable fluid. Humeral head (*double arrowheads*) is to the left, hyperechoic glenoid labrum (*single arrowhead*) and infraspinatus muscle and tendon (*arrows*) are to the right.

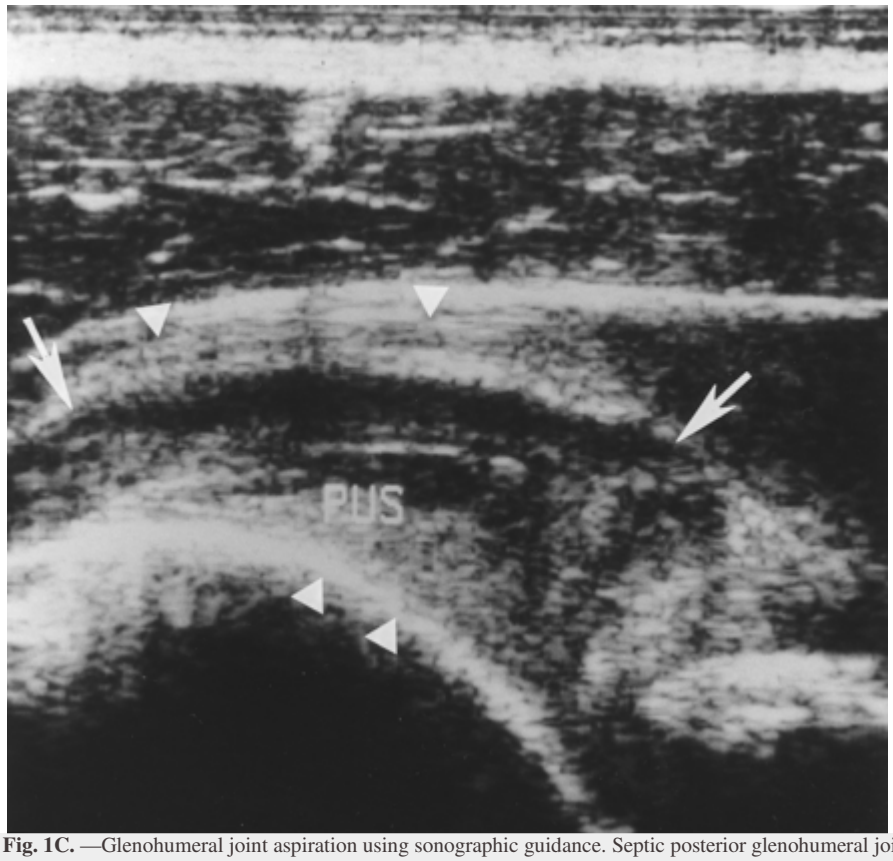

Fig. 1C. —Glenohumeral joint aspiration using sonographic guidance. Septic posterior glenohumeral joint. Sonogram obtained as illustrated in **A** shows hypoechoic joint effusion (*arrows*) displacing infraspinatus tendon (*single arrowheads*). Humeral head (*double arrowheads*) is to the left. Culture of aspirate grew *Staphylococcus aureus*.

When aspiration under sonographic guidance is chosen, the needle is advanced at an angle along the long axis of the transducer and appears as a bright echogenic line. If the needle axis approaches 90° to the ultrasound beam, reverberation artifacts may be seen posterior to the needle [1]. If the needle is advanced transverse to the axis of the transducer, an echogenic dot or short linear component may be visualized. The needle is usually well visualized in a cystic fluid collection [1]. Maneuvers to aid visualization of the needle include gentle movement of the needle (side to side or in and out), injection of a small amount of saline or air, and movement of the stylet to and fro within the needle [1]. Power Doppler sonography detects motion and can also be applied to aid detection of the needle tip during advancement.

In cases in which a high clinical suspicion exists for a joint infection but only a borderline or minimal effusion is detected on sonography, sterile, nonbacteriostatic saline can be injected and reaspirated for analysis. Comparison with the contralateral, asymptomatic joint aids evaluation when there is a question of a small effusion, though asymmetry of joint fluid does not always imply an abnormal effusion [5]. Scanning after aspiration can assess residual or loculated fluid collections.

As with traditional arthrography, potential complications include vasovagal reaction, puncture of neurovascular structures, iatrogenic infection, and failure to aspirate joint fluid. Whenever possible, aspiration should be performed with the patient supine to decrease the potential complications of a vasovagal reaction. Visual assessment and close communication with the patient during the procedure aid assessment for a vasovagal reaction. Knowledge of the neurovascular anatomy along with sonographic assessment, including Doppler evaluation, allows avoidance of the neurovascular structures. Iatrogenic infection is extremely rare when proper technique is used [6]. Failure to aspirate joint fluid is most often caused by an inaccurate skin marking or confusion of hypoechoic synovitis with an effusion.

Shoulder

Sonographic guidance of needle placement during MR arthrography of the shoulder has been described for both the anterior [7] and posterior [8] approaches. The posterior approach is frequently used because fluid generally accumulates first in the infraspinatus recess of the posterior glenohumeral joint [1] (Fig. 1A,1B,1C). Dynamic posterior scanning during adduction or abduction can aid in detecting small effusions. For the posterior approach, aspiration is performed with the patient sitting upright. Close monitoring for any signs of a vasovagal reaction is mandatory. The joint capsule is punctured along the medial border of the humeral head, slightly lateral to the glenohumeral joint. This approach avoids contact with the suprascapular nerve and circumflex scapular vessels that course medial to the glenoid rim [9]. Using this approach, Cicak et al. [8] reported successful and uncomplicated sonographic needle placement for arthrography in 24 patients. We have routinely used the posterior approach without complication.

The anterior approach is similar to the approach used in standard arthrography. The patient is supine, and the entry site is a central line between the coracoid and the anteromedial humeral head when scanning axially [7]. The entry site must be lateral to the coracoid to avoid major neurovascular structures including the cephalic vein, axillary artery, and brachial plexus [9]. The needle tip can be visualized adjacent to the cartilage of the humeral head on axial imaging [7]. Using this approach, Valls and Melloni [7] reported successful and uncomplicated sonographic needle placement for arthrography in 50 patients. Typically, we would use an anterior approach if fluid is noted only anteriorly (and not posteriorly), or if the patient must remain supine.

Extraarticular fluid collections, including subacromial and subdeltoid bursal fluid, acromioclavicular joint fluid, and soft-tissue abscess, can also be identified and aspirated using sonographic guidance (Fig. 2A,2B). Such noncommunicating fluid collections would not be detected by fluoroscopic aspiration of the glenohumeral joint and may not be detected by physical examination. Transducer and needle positioning for aspiration of bursa are variable, depending on the location of the greatest amount of fluid.

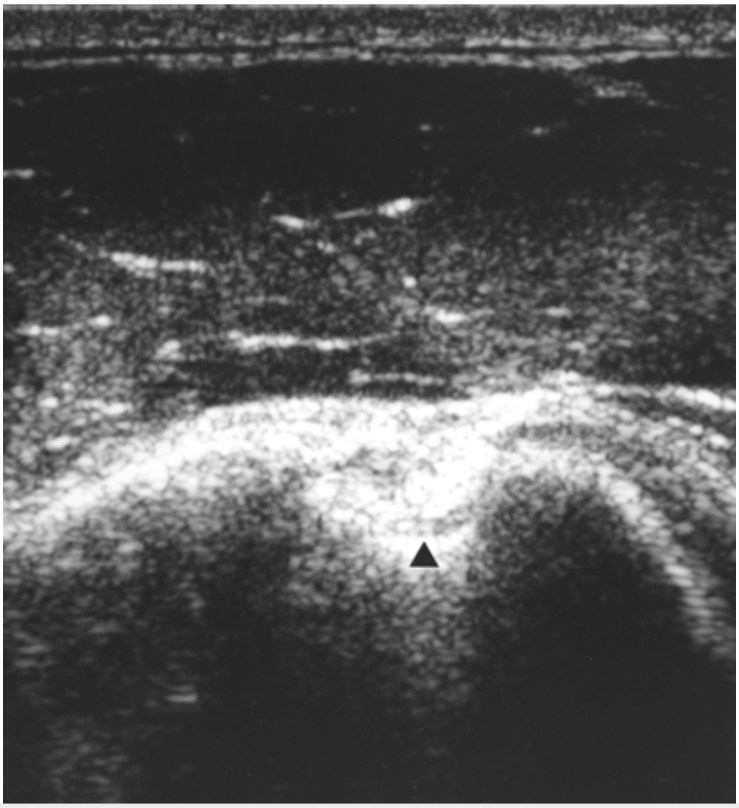

Fig. 2A. —Subacromial and subdeltoid bursae aspiration using sonographic guidance. Sonogram of normal anterior shoulder transverse to biceps tendon. Note absence of fluid in subacromial and subdeltoid bursae. Biceps tendon is seen in bicipital groove of humerus (*arrowhead*).

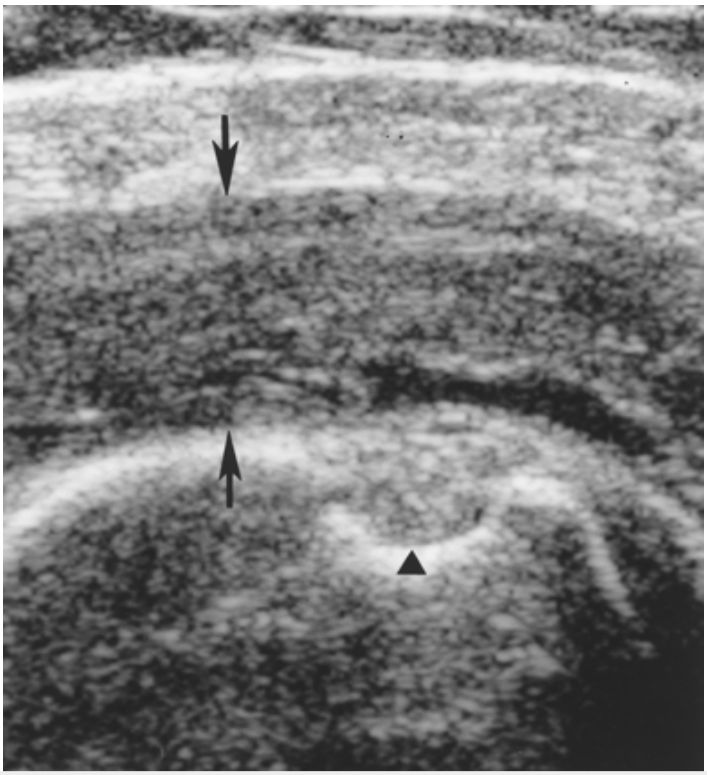

Fig. 2B. —Subacromial and subdeltoid bursae aspiration using sonographic guidance. 45-year-old woman in whom a septic glenohumeral joint was suspected on clinical grounds. Sonogram of anterior shoulder transverse to biceps tendon shows heterogeneous fluid collection in subacromial and subdeltoid bursae (*arrows*). Biceps tendon is seen in bicipital groove (*arrowhead*). Aspiration of bursa was performed from anterior approach at level of biceps groove. Culture grew *Pseudomonas aeruginosa*. No fluid was identified in glenohumeral joint (not shown).

Elbow

We frequently use the posterior approach for joint aspiration of the olecranon recess [1] (Fig. 3A,3B,3C). Evaluation of the olecranon recess in the flexed elbow is the optimal approach for sonographic detection of an effusion [10] (Fig. 3C). The absence of major neurovascular structures in the posterior elbow at the level of the triceps tendon allows a safe approach. We have found the posterior approach to be rapid and without complication.

Fig. 3A. —Elbow joint aspiration using sonographic guidance. Photograph shows transducer positioning for posterior transverse sonography of olecranon fossa and needle positioning for aspiration. For purposes of illustration, sterile transducer cover and drape are not shown.

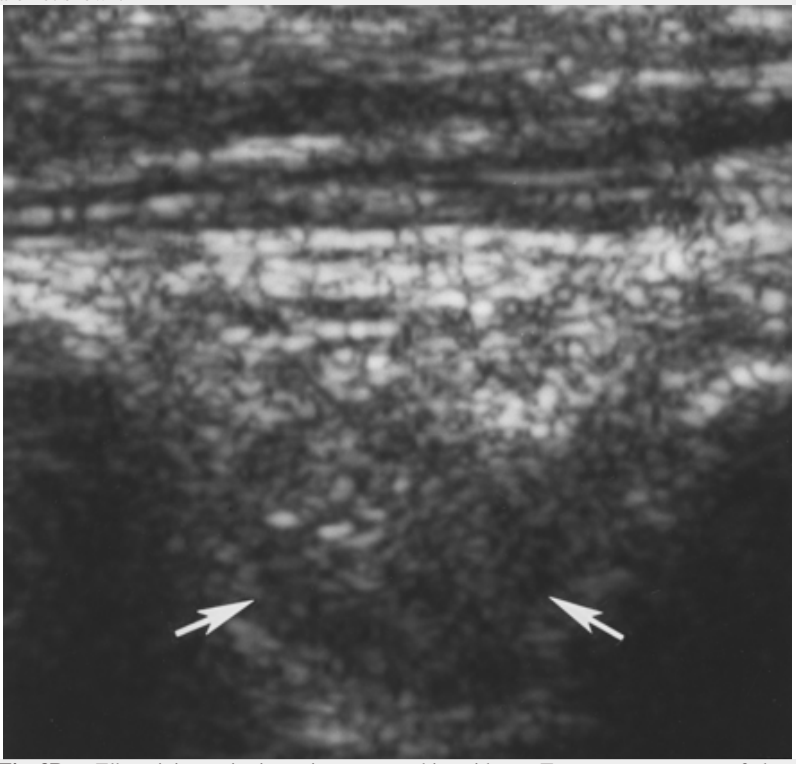

Fig. 3B. —Elbow joint aspiration using sonographic guidance. Transverse sonogram of olecranon fossa, scanned as illustrated in **A**, shows no detectable fluid. Arrows mark olecranon fossa at posterior aspect of distal humerus.

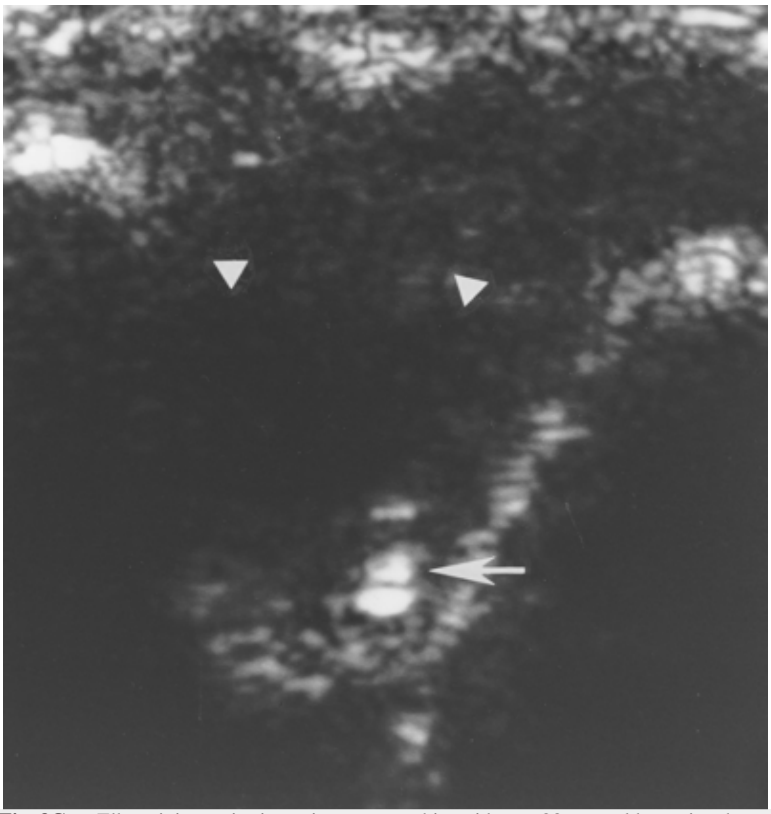

Fig. 3C. —Elbow joint aspiration using sonographic guidance. 23-year-old man in whom septic elbow effusion was suspected on clinical grounds. Transverse sonogram shows tip of needle (*arrow*) in fluid collection (*arrowheads*). Because aspiration was performed with needle perpendicular to long axis of transducer (**A**), only tip of needle is visualized

Joint aspiration can also be performed from an anterolateral approach, as with standard arthrography, with the needle tip placed in the radio-capitellar joint [1, 11]. This approach can be more difficult and time-consuming because the needle tip must be placed in a smaller space.

Hip

Sonography is frequently used for evaluation of hip effusions in both the adult and pediatric population [2, 6]. For evaluation of the hip, the patient is supine with the hip in extension and slight abduction [12]. The transducer is oriented anteriorly along the axis of the femoral neck (Fig. 4A,4B,4C,4D).

Fig. 4A. —Hip joint aspiration using sonographic guidance. Photograph shows transducer positioning for longitudinal sonography of hip and needle positioning for aspiration. For purposes of illustration, sterile transducer cover and drape are not shown.

Fig. 4B. —Hip joint aspiration using sonographic guidance. Sonography of normal hip joint. Longitudinal sonogram of normal hip joint longitudinal to femoral neck. Acetabulum is to the left, and arrowheads mark femoral head and shaft. No fluid is seen distending joint capsule.

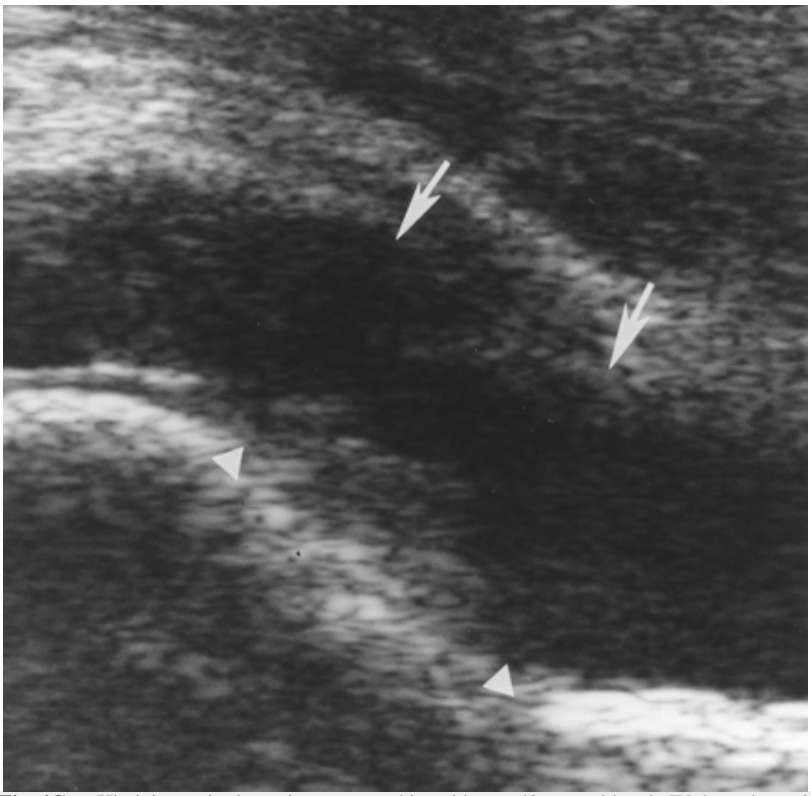

Fig. 4C. —Hip joint aspiration using sonographic guidance. 42-year-old male IV drug abuser in whom septic hip joint was clinically suspected. Longitudinal sonogram obtained as illustrated in **A** shows hypoechoic hip effusion between arrowheads marking femoral cortex and corresponding arrows marking joint capsule. Culture of aspirate grew *Staphylococcus aureus*

Fig. 4D. —Hip joint aspiration using sonographic guidance. 74-year-old man with increasing hip pain after hemiarthroplasty. Longitudinal sonogram of hypoechoic hip effusion noted between arrowhead marking hip prosthesis and corresponding long arrow marking joint capsule. Bone-to-capsule distance, measured between short arrows, is 11 mm. Note reverberation artifact posterior to metal components (*curved arrow*).

The femoral artery is palpated or localized with sonography and marked for reference, and aspiration is performed at least 1 cm lateral to the neurovascular bundle. The needle tip can be visualized in the capsule, adjacent to the femoral neck. With proper technique, iatrogenic hip infections caused by joint aspiration are very rare, reported in zero of 800 aspirations [6].

Hip effusions are seen as fluid that displaces the capsule away from the echogenic cortex of the femoral neck [2, 6] (Fig. 4C). A difference in joint distention of greater than or equal to 2 mm between the symptomatic and

asymptomatic hip has been reported as significant [2]. Thickening of the capsule (≥2 mm) and changes in the cortex of the proximal femur have also been reported with septic arthritis [2].

Sonography has also been used to detect joint effusions and extraarticular fluid collections in patients with hip prostheses (Fig. 4D). An effusion with a bone-to-capsule distance greater than or equal to 3.2 mm with a concomitant extraarticular fluid collection has been reported as highly specific for infection [13]. Periarticular fluid collections in such cases may have originally communicated with the joint, with subsequent "walling off" of the periarticular collection, or such collections could be due to a second nidus of infection (in addition to the joint infection).

Extraarticular fluid collections such as greater trochanteric bursitis can also be detected and aspirated using sonographic guidance (Fig. 5). The location of the fluid and major neurovascular structures determines the aspiration approach. Typically, a lateral approach is used for aspiration of the greater trochanteric bursa. Such fluid collections would not be detected by blind or fluoroscopic aspiration of the hip and may not be detected on physical examination.

Fig. 5. —68-year-old woman with clinical concern for septic hip after hemiarthroplasty. Transverse sonogram over greater trochanteric bursa shows hypoechoic fluid collection (*arrowheads*). Arrows mark echogenic cortex of greater trochanter. Hip joint (not shown) showed no fluid. Using fluoroscopic or traditional "blind" aspiration, this fluid would not have been detected and patient would have endured an unsuccessful attempt at joint aspiration

Knee

The patient is examined supine with the knee extended and the popliteal fossa flush with the examination table (Fig. 6A,6B,6C,6D,6E). Longitudinal scanning over the distal quadriceps tendon just proximal to the patella is used to assess the suprapatellar bursa. A small amount of fluid is physiologic and is usually first noted in the lateral recess (Fig. 6B). Larger amounts that distend the suprapatellar bursa are easily detected and are abnormal (Fig. 6C).

Fig. 6A. —Knee joint aspiration using sonographic guidance. Evaluation for effusion. Photograph shows transducer positioning for longitudinal scanning of suprapatellar bursa to evaluate for joint effusion. Longitudinal imaging is easiest for detection of fluid. However, bony anatomy of patella obstructs needle placement in longitudinal orientation. Therefore, transverse orientation is used for aspiration when sonographic guidance is required.

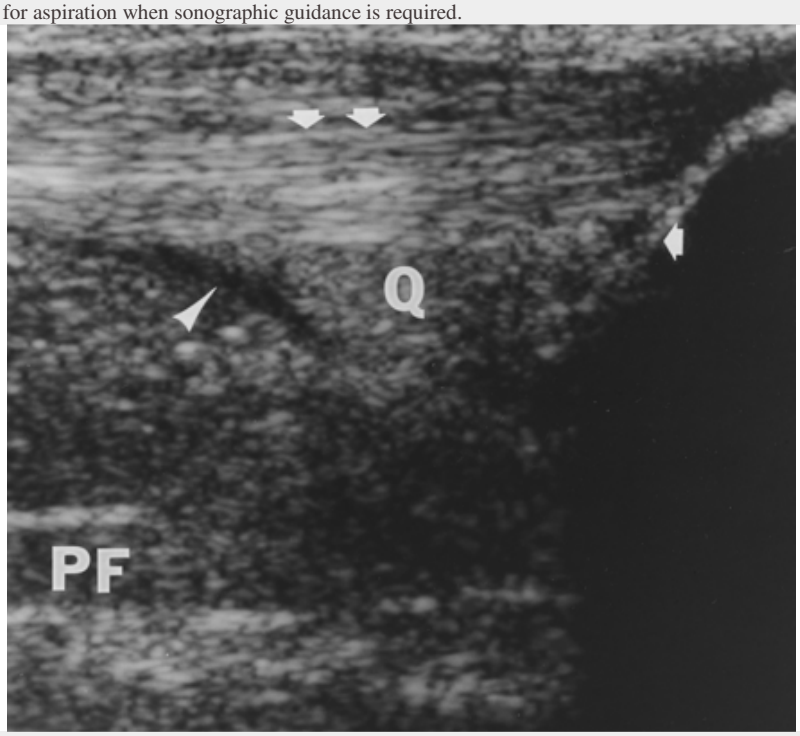

Fig. 6B. —Knee joint aspiration using sonographic guidance. Longitudinal sonogram of normal suprapatellar bursa shows physiologic amount of fluid (*arrowhead*). Patella is to the right (*single arrow*) and quadriceps tendon is seen superficially (*double arrows*). Note hyperechoic prefemoral (PF) and quadriceps (Q) fat pads

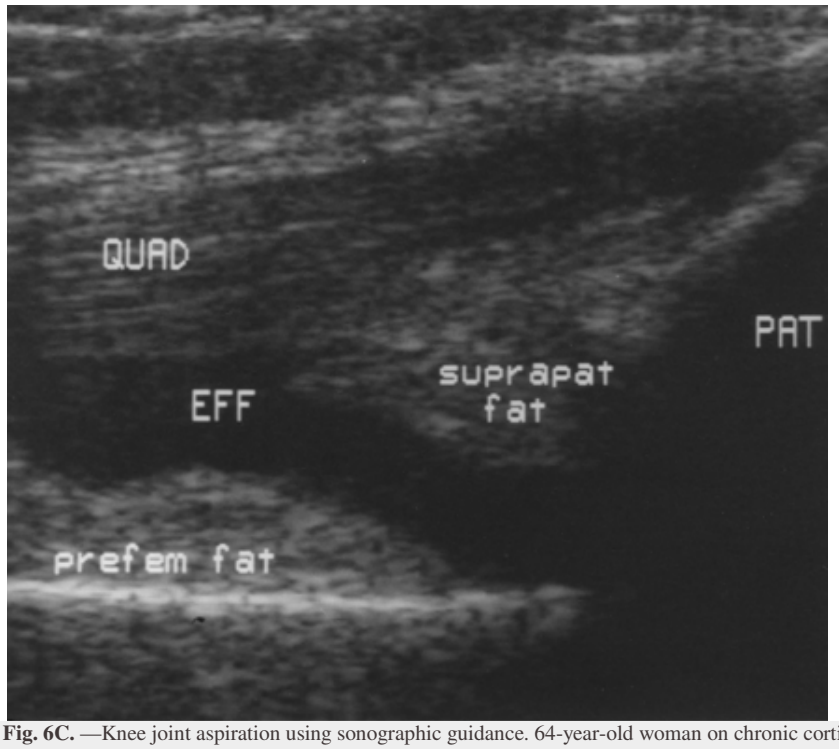

Fig. 6C. —Knee joint aspiration using sonographic guidance. 64-year-old woman on chronic corticosteroid treatment in whom ruptured quadriceps tendon was suspected on clinical grounds. Longitudinal sonogram shows hypoechoic effusion (EFF) in suprapatellar bursa. Suprapatellar and prefemoral fat are labeled. PAT = patella, QUAD = intact quadriceps tendon.

Fig. 6D. —Knee joint aspiration using sonographic guidance. Joint aspiration using sonographic guidance. Photograph shows transducer positioning for transverse sonography of suprapatellar bursa and needle positioning for aspiration. For purposes of illustration, sterile transducer cover and drape are not shown.

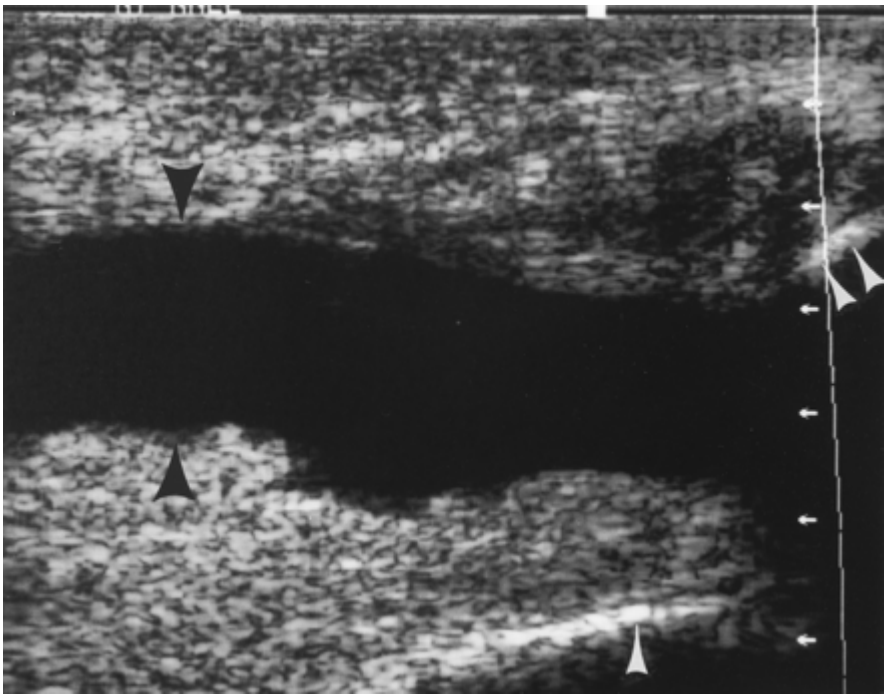

Fig. 6E. —Knee joint aspiration using sonographic guidance. 43-year-old woman in whom septic knee effusion was clinically suspected. Transverse sonogram shows hypoechoic effusion in suprapatellar bursa (*black arrowheads*). Note femoral cortex (*single white arrowhead*) and patellar cortex (*double white arrowheads*).

Longitudinal imaging is the easiest for detection of fluid (Fig. 6A). However, the bony anatomy of the patella obstructs needle placement in the longitudinal orientation. Therefore, the transverse orientation is used for aspiration when sonographic guidance is required (Fig. 6D). Aspiration can be performed from an anterolateral or anteromedial approach depending on the location of the fluid. No major neurovascular structures are encountered by these approaches. The tip of the needle can be visualized in the suprapatellar bursa. Extraarticular fluid collections, including abscesses and bursal fluid collections, can also be detected and aspirated with sonographic guidance (Figs. 7 and 8).

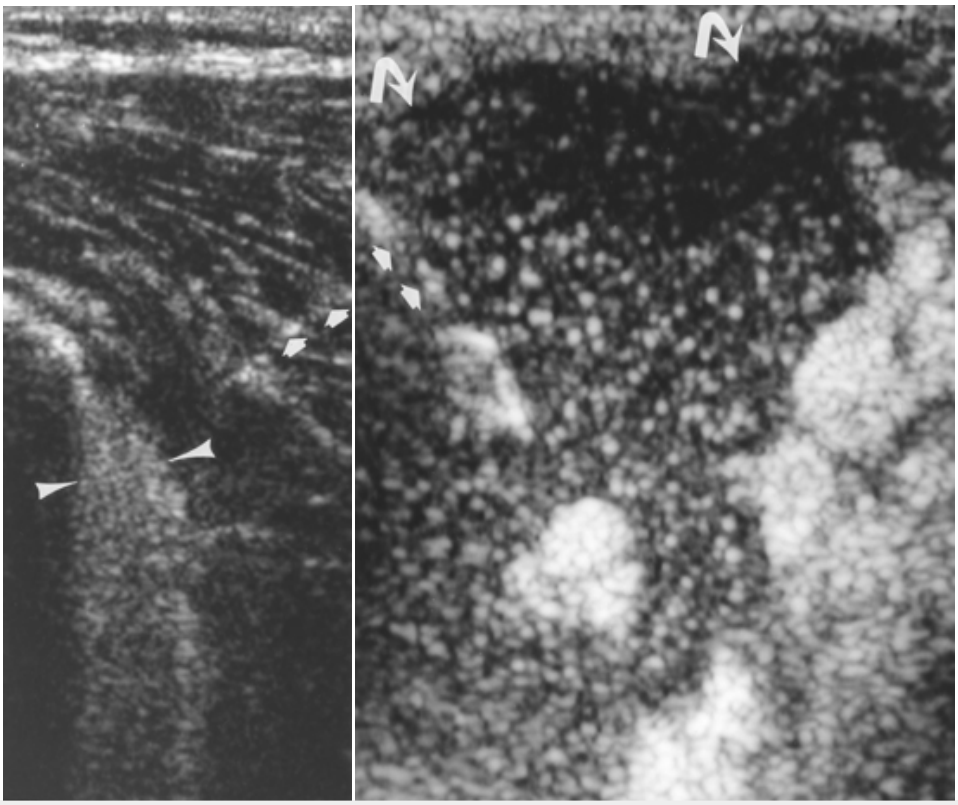

Fig. 7 (Left) —21-year-old man with sickle cell anemia and distal femoral fluid collection seen on MR imaging (not shown). Transverse sonogram of distal femur shows echogenic fluid collection (*arrowheads*) and aspiration needle (*arrows*). Analysis of aspirate yielded >100,000 WBC/ml without identification of an organism, likely a result of antibiotic therapy.

Fig. 8. (right)—75-year-old man with cellulitis surrounding knee in whom clinical findings suggested soft-tissue fluid collection. Transverse sonogram of lateral knee shows complex fluid in lateral knee bursa (*curved arrows*) and aspiration needle (*straight arrows*). Analysis of aspirate revealed Gram-positive cocci.

Ankle

An ankle joint effusion is optimally detected with the ankle in plantar flexion [14] (Fig. 9A,9B,9C). Up to 3 mm (anteroposterior dimension) of joint fluid has been observed in normal volunteers and can be asymmetric when compared with the opposite ankle [2]. An effusion is seen as anechoic or hypoechoic joint fluid that distends the anterior recess (Fig. 9C).

Fig. 9A. —Ankle joint aspiration using sonographic guidance. Photograph shows transducer positioning for longitudinal sonography of tibiotalar joint and needle positioning for aspiration. Ankle is placed in plantar flexion to aid detection and aspiration. For purposes of illustration, sterile transducer cover and drape are not shown.

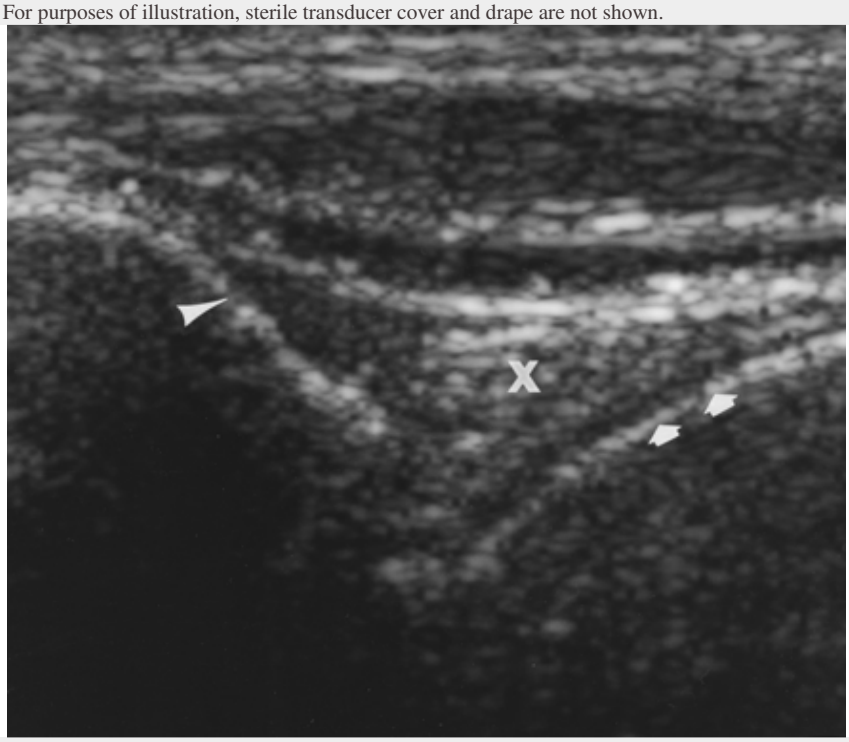

Fig. 9B. —Ankle joint aspiration using sonographic guidance. Longitudinal sonogram of normal anterior ankle joint shows tibia to left (*arrowhead*) and talus to right (*arrows*). No fluid is detected. Note hyperechoic fat pad (X).

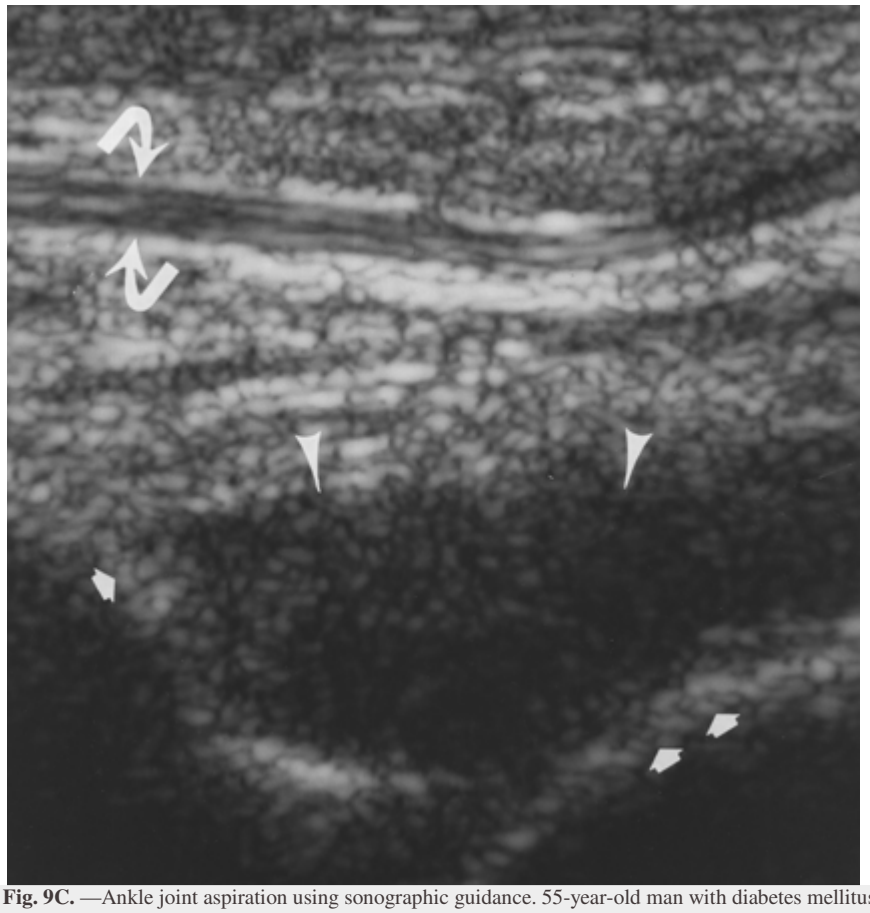

Fig. 9C. —Ankle joint aspiration using sonographic guidance. 55-year-old man with diabetes mellitus in whom septic tibiotalar joint was suspected on clinical grounds. Longitudinal sonogram shows hypoechoic tibiotalar joint effusion (*arrowheads*). Analysis of aspirate revealed uric acid crystals, confirming diagnosis of gout. Note tibia (*single straight arrow*), talus (*double straight arrows*), and extensor tendon (*curved arrows*).

Before aspiration, the dorsalis pedis artery is localized by sonography. An anterior entry site for aspiration is chosen medially or laterally to avoid the artery and adjacent deep peroneal nerve (located immediately lateral to the artery). The tip of the needle can be visualized adjacent to the hypoechoic cartilage of the tibiotalar joint.

Septic tenosynovitis of the extensor tendons can also be seen with sonographic evaluation (Fig. 10). Blind or fluoroscopic aspiration of the joint through septic tenosynovitis could infect an aseptic joint and can be avoided with sonographic evaluation.

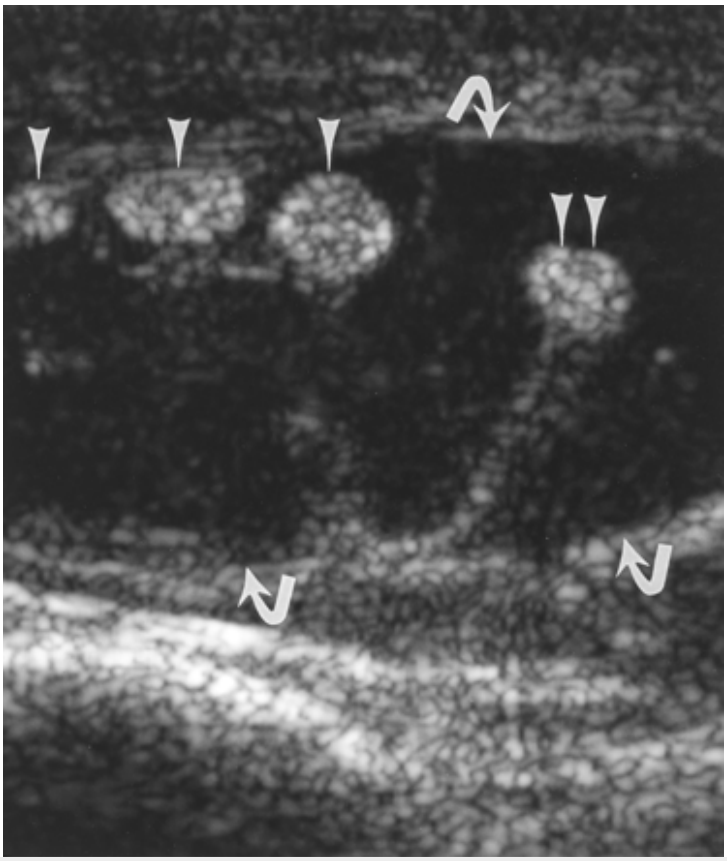

Fig. 10. —82-year-old woman with diabetes mellitus and clinical findings suggesting ankle effusion. Transverse sonogram of extensor digitorum tendons (*single arrowheads*) and peroneus tertius (*double arrowheads*) shows complex fluid surrounding tendons (*curved arrows*). Culture of aspirate grew *Nocardia asteroides*. Fluoroscopic or "blind" aspiration of ankle joint through this septic tenosynovitis could have infected an aseptic ankle joint.

Conclusion

With sonographic evaluation, attempted aspiration of a dry joint can be avoided. The number of punctures needed to obtain a diagnostic sample may also be decreased. The use of sonography allows identification and aspiration of extraarticular fluid collections, including abscesses and bursitis. Contamination of an aseptic joint by fluoroscopic arthrocentesis through an undiagnosed abscess, septic bursitis, or septic tenosynovitis can be prevented. With sonographic guidance, the optimal access route to the fluid can be chosen to ensure a safe and successful aspiration.

References

1. *Cardinal E, Chhem RK, Beauregard CG. Ultrasound-guided interventional procedures in the musculoskeletal system. Radiol Clin North Am 1998;36:597 -604* CrossRefMedline

2. *Shiv VK, Jain AK, Taneja K, Bhargava SK. Sonography of hip joint in infective arthritis. Can Assoc of Radiol J 1990;41:76 -78*

3. *Strouse PJ, DiPietro MA, Adler RS. Pediatric hip effusions: evaluation with power Doppler sonography. Radiology 1998;206:731 -735* Abstract/FREE Full Text

4. *Breidahl WH, Stafford-Johnson DB, Newman JS, et al. Power Doppler sonography in tenosynovitis: significance of the peritendinous hypoechoic rim. J Ultrasound Med 1998;17:103 -107* Abstract

5. *Nazarian LN, Rawool NM, Martin CE, Schweitzer ME. Synovial fluid in the hindfoot and ankle: detection of amount and distribution with US. Radiology 1995;197:275 -278* Abstract/FREE Full Text

6. *Berman L, Fink AM, Wilson D, McNally E. Technical note: identifying and aspirating hip effusions. Br J Radiol 1995;68:306 -310* Abstract/FREE Full Text

7. *Valls R, Melloni P. Sonographic guidance of needle position for MR arthrography of the shoulder. AJR 1997;169:845 -847* FREE Full Text

8. *Cicak N, Matasovic T, Bajraktarevic T. Ultrasonographic guidance of needle placement for shoulder arthrography. J Ultrasound Med 1992;11:135 -137* Abstract

9. *Hulstyn MJ, Fadale PD. Arthroscopic anatomy of the shoulder. Orthop Clin North Am 1995;26:597 -612* Medline

10. *De Maeseneer M, Jacobson JA, Joavisidha S, et al. Elbow effusions: distribution of joint fluid with flexion and extension and imaging implications. Invest Radiol 1998;33:117 -125* CrossRefMedline

11. *Cardinal E. In: Hodge JC, ed. Musculoskeletal imaging: diagnostic and therapeutic procedures. Basel, Switzerland: Karger Landes, 1997: 237*

12. *Chan YL, Cheng JC, Metreweli C. Sonographic evaluation of hip effusion in children: improved visualization with the hip in extension and abduction. Acta Radiol 1997;38:867 -869* Medline

13. *van Holsbeeck MT, Eyler WR, Sherman LS, et al. Detection of infection in loosened hip prostheses: efficacy of sonography. AJR 1994;163:381 -384* Abstract/FREE Full Text

14. *Jacobson JA, Andresen R, Jaovisidha S, et al. Detection of ankle effusions: comparison study in cadavers using radiography, sonography, and MR imaging. AJR 1998;170:1231 -1238* Abstract/FREE Full Text

O outro artigo citado foi Am J Sports Med. 2005 Feb;33(2):255-62.

A prospective, double-blind, randomized clinical trial comparing subacromial injection of betamethasone and xylocaine to xylocaine alone in chronic rotator cuff tendinosis.

Alvarez CM, Litchfield R, Jackowski D, Griffin S, Kirkley A.

Source - B.C. Children's Hospital, Vancouver, Canada.

Abstract

BACKGROUND:

Rotator cuff tendinosis is a common problem with significant health and economic effects. Nonoperative management includes the widespread use of subacromial steroid injections despite the lack of evidence of its efficacy.

HYPOTHESIS:

A subacromial injection of betamethasone will be more effective than xylocaine alone in improving the quality of life, impingement sign, and range of motion in patients who have chronic rotator cuff tendinosis or partial rotator cuff tears.

STUDY DESIGN:

Randomized controlled clinical trial; Level of evidence, 1.

METHODS:

Patients with rotator cuff tendinosis or partial cuff tear with symptoms longer than 6 months, with failure of 6 weeks of physical therapy and 2 weeks of nonsteroidal anti-inflammatory drugs, who were older than 30 years of age, and who showed >50% improvement with the Neer impingement test were stratified for Workplace Safety and Insurance Board status and previous injection. Outcome measures--the Western Ontario Rotator Cuff Index; American Shoulder and Elbow Surgeons standardized form; Disabilities of the Arm, Shoulder and Hand; active forward elevation; active internal rotation; active external rotation; and the Neer impingement sign--were assessed at 2, 6, 12, and 24 weeks after injection. The injection into the subacromial space contained either 5 mL of 2% xylocaine alone or 4 mL of 2% xylocaine and 1 mL (6 mg) of betamethasone in an opaque syringe.

RESULTS:

In 58 patients (betamethasone group, n = 30; xylocaine group, n = 28), the authors found no statistically significant difference between the 2 treatment groups for all outcomes and time intervals. The scores for the Western Ontario Rotator Cuff Index at 3 months were xylocaine = 45.4% +/- 13% and betamethasone = 56.3% +/- 17% (P = .13). At 6 months, the scores were xylocaine = 51% +/- 32% and betamethasone = 59% +/- 26% (P = .38). All other outcomes showed similar values. As well, similar results were found for 2 and 6 weeks after injection. Both groups showed improvement from baseline in all outcomes.

CONCLUSIONS:

With the numbers available for this study, the authors found betamethasone to be no more effective in improving the quality of life, range of motion, or impingement sign than xylocaine alone in patients with chronic rotator cuff tendinosis for all follow-up time intervals evaluated.

O autor concluiu que a injeção de esteróide na terapia músculo esquelética é útil. O direcionamento US na injeção torna mais precisa a localização do local a ser tratado e reduz as complicações decorrentes das injeções de esteróide.

O FUTURO DO US MÚSCULO ESQUELÉTICO DA PERSPECTIVA DO FÍSICOS

Ministrada pelo Dr. Tomy Varghese, PhD - pesquisa patrocinada pelo INH - instituto nacional da saúde dos EUA

O autor menciona que a US provê imagens em tempo real dos tecidos e estruturas se movimentando, o que é essencial no diagnóstico músculo esquelético e, na maioria das vezes, oferece imagens melhores da estrutura do tendão. O fato do sistema atuais de US serem bem menores e portáteis significou grande avanço para o US músculo esquelético. É também o método de escolha para procedimentos minimamente invasivos, tal como a biópsia e a aspiração com agulha dirigida pelo US, que é uma área relativamente nova de aplicação da US em

procedimentos músculo esqueléticos. Os US portáteis estão rapidamente ganhando aplicação na área músculo esquelética, principalmente por suas imagens darem diagnósticos imediatos de injúrias no esporte e por permitir aplicações terapêuticas em pontos específicos. A evolução dos US portáteis, que melhoraram os canais disponíveis e a sua capacidade de operar com sondas de alta freqüência, tem ajudado significantemente as aplicações nas imagens músculo esqueléticas. Esta evolução foi possível pela extrema miniaturização dos componentes eletrônicos digitais. Entretando, a miniaturização dos circuitos eletrônicos analógicos para os estágios de pré amplificação e alguns componentes eletrônicos específicos da imagem US têm evoluído mais lentamente. Os avanços nos softwares dos componentes formadores do feixe US têm sido outra tendência e que evoluiu para uma arquitetura eletrônica mais flexível dos sistemas. A migração de muitas das funções dos formadores de feixe para componentes eletrônicos dentro da caixa do transdutor podem eventualmente resultar num sistema robusto de sonda US sem fio com dispositivos manuais que exibem a tela de US. Muitos fabricantes estão anunciando esses sistemas portáteis com um transdutor conectado com um processador de imagem analógico ou digital que possa ser carregado na mão e mostrar a tela. A resolução espacial e melhora da penetração com as aquisições compostas excitação codificada, emissão de feixes de estimulação codificados e a imagem harmônica foram discutidas durante a palestra.. A geração das sondas com harmônicas, nas quais se usa a propriedade de selecionar uma freqüência para ser utilizada dentre as muitas emitidas pelo feixe ultrassonográfico pulsátil, pois ele se distorce gradualmente, a medida que se propaga nos tecidos. Este é o motivo pelo qual as harmônicas só podem ser utilizadas nos tecidos mais profundos, pois elas aumentam proporcionalmente a profundidade. A excitação codificada melhora muito a imagem. O feixe contém diferentes freqüências de pulsos:

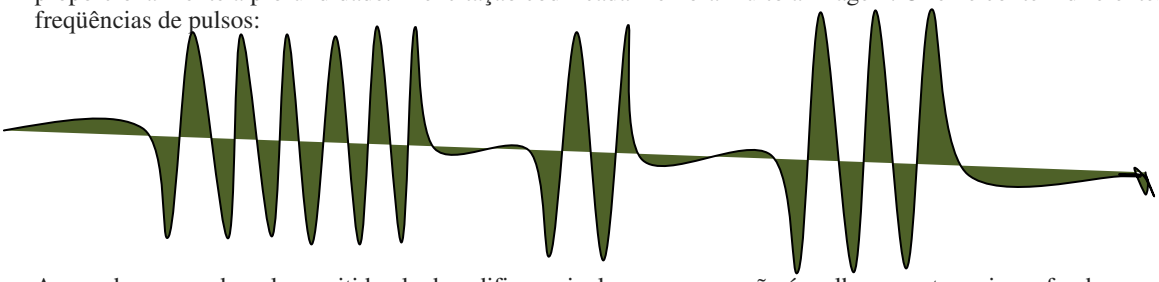

Ao receber o eco do pulso emitido ele decodifica o sinal e essa percepção é melhor quanto mais profunda estiver situada a estrutura ou lesão.

O US composto espacial consegue diminuir o pontilhamento da imagem. Ele mencionou um artigo publicado no AM. J Roentgenol, 2002; 179:1629-1631:

Advantages of Real-Time Spatial Compound Sonography of the Musculoskeletal System Versus Conventional Sonography

1. **Dennis C. Lin[1], Levon N. Nazarian[1], Patrick L. O'Kane[1], John M. McShane[2], Laurence Parker[1] and Christopher R. B. Merritt[1]**

Abstract

OBJECTIVE. Spatial compound sonography is a method that obtains sonographic information from several different angles of insonation and combines them to produce a single image. By reducing speckle and improving definition of tissue planes, this method can potentially improve image quality in musculoskeletal sonography. The purpose of our study was to compare real-time spatial compound sonography with conventional high-resolution musculoskeletal sonography.

MATERIALS AND METHODS. Thirty-four patients underwent sonography of the musculoskeletal system for a variety of indications. All patients were evaluated using conventional high-resolution sonography and real-time spatial compound sonography performed with a 12-5-MHz multifrequency linear array transducer. Conventional images and compound images depicting the same musculoskeletal structure were obtained in pairs. A total of 118 images (59 image pairs) were randomly assorted and reviewed on a computer monitor by three experienced sonologists working independently. The reviewers were unaware of the type of images they

were evaluating. Image quality was rated using a 5-point scale. The image parameters evaluated were definition of tissue planes, speckle, other noise, and image detail.

RESULTS. Analysis of variance revealed that real-time spatial compound sonography significantly improved definition of soft-tissue planes, reduced speckle and other noise, and improved image detail when compared with conventional high-resolution sonography ($p < 0.0001$ for all evaluated parameters).

CONCLUSION. Real-time spatial compound sonography significantly improved sonographic image quality in the musculoskeletal system when compared with conventional high-resolution sonography. Because musculoskeletal sonography is highly dependent on image quality and tissue-plane definition, spatial compound sonography represents an important development.

Introduction

Spatial compound sonography is a method in which sonographic information is obtained from several different angles of insonation and combined to produce a single image [1,2,3,4]. This technique is unlike conventional B-mode sonography, in which each image is obtained from a single angle of insonation. By averaging images from multiple angles of insonation, spatial compound sonography has been shown to reduce many image artifacts inherent in conventional sonography [3,4].

The concept of compound sonography has been around since the 1960s. However, it was not until recently—with advances in computing power and image processing—that real-time spatial compound sonography became a reality. As a result, there has been renewed interest in this technique. Recently, spatial compound sonography has been shown to improve image quality in a variety of settings ranging from sonography of the breast [5] to the thyroid [6] and atherosclerotic plaque [7].

In this study, we investigated whether spatial compound sonography improves tissue-plane definition, speckle, noise, and detail—all crucial factors in interpreting musculoskeletal sonography.

Previous SectionNext Section

Materials and Methods

The study group was composed of 34 consecutive patients undergoing sonography of the musculoskeletal system for various indications between June 21, 2000, and February 28, 2001. The mean age of patients was 40 years, with ages ranging from 15 to 75 years. Nineteen patients were male and fifteen were female. No patients were excluded from the study. Eight patients were referred for lateral epicondylitis of the elbow, whereas another seven were referred for tears of various upper and lower extremity muscles. Six patients were referred for patellar tendinopathy, and six, for tendinopathy elsewhere. The remaining seven patients had a miscellany of other diagnoses. Each patient was evaluated with both conventional high-resolution sonography and real-time spatial compound sonography. Images were obtained by an experienced sonographer using a 12-5-MHz multifrequency linear array transducer on an HDI 5000 scanner (Advanced Technology Laboratories, Bothell, WA). The sonographer was instructed to obtain images of any pathologic change and images in which normal anatomy was well depicted. Conventional images and compound images were obtained in pairs, with each image in the pair depicting the same musculoskeletal structure. A total of 118 images (59 image pairs) were obtained.

The images were then scanned using a Duoscan HiD scanner (Agfa, Wilmington, MA), randomly assorted, and displayed on a computer monitor using FileMaker Pro 5.0 software (FileMaker, Santa Clara, CA). All images were reviewed independently by three experienced sonologists who were unaware of the type of images they were evaluating. Each image was rated for definition of tissue planes, amount of speckle and other noise, and image detail using a 5-point scale: 1, unacceptable; 2, poor quality but marginally acceptable; 3, fair quality and acceptable; 4, good quality; and 5, excellent or outstanding quality. Speckle was defined as the granular appearance of a sonographic image that results from the constructive and destructive interaction of acoustic fields from the scattering of the ultrasound beam from small tissue reflectors [5]. Noise was defined as all other artifacts degrading image quality, including clutter and blurring caused by motion. A three-way analysis of

variance for each of these variables was performed to account for differences in image type (conventional versus compound), reviewers, and the body part of the patient scanned. Institutional review board approval was obtained for this retrospective analysis.

Results

An analysis of variance revealed that real-time spatial compound sonography significantly improved definition of soft-tissue planes, reduced speckle and other noise, and improved image detail when compared with conventional high-resolution sonography ($p < 0.0001$ for all evaluated parameters).

Regarding definition of tissue planes, conventional images received a mean score (± SD) of 2.88 ± 0.97, whereas the mean score for compound images was 3.67 ± 1.08. For speckle, conventional and compound images received mean scores of 2.74 ± 1.04 and 4.01 ± 0.9, respectively. For all other noise, conventional and compound images received mean scores of 2.87 ± 0.94 and 3.86 ± 1.02, respectively. Finally, for detail, conventional and compound images received mean scores of 2.98 ± 0.90 and 3.84 ± 0.96, respectively.

Discussion

Sonographic evaluation of the musculoskeletal system is unlike imaging of other organ systems. This difference is due in large part to the anisotropic nature of muscles and tendons. Most organs in the body (e.g., liver and kidney) are composed of diffuse reflectors that scatter the ultrasound beam and give these organs their homogeneous sonographic appearance. However, muscles and tendons are composed primarily of specular reflectors. When this type of reflector is insonated, the amplitude of the echo is highly dependent on the angle of incidence. The greatest amplitude is achieved when the ultrasound beam is perpendicular to this reflector. For example, the fibrillar pattern of a tendon is best appreciated when the ultrasound beam is perpendicular to the tendon and becomes less distinct at other angles of insonation.

In this study, spatial compounding was shown to improve tissue-plane definition. This improvement is likely due in part to the fact that images are acquired from multiple angles. As the image is generated from more angles of insonation, the likelihood is greater that one of these angles will be perpendicular to specular reflectors, generate a higher echo amplitude, and thereby reduce anisotropic effects (Fig. 1A,1B). Curved surfaces thus appear more continuous and tissue-plane definition is improved [8].

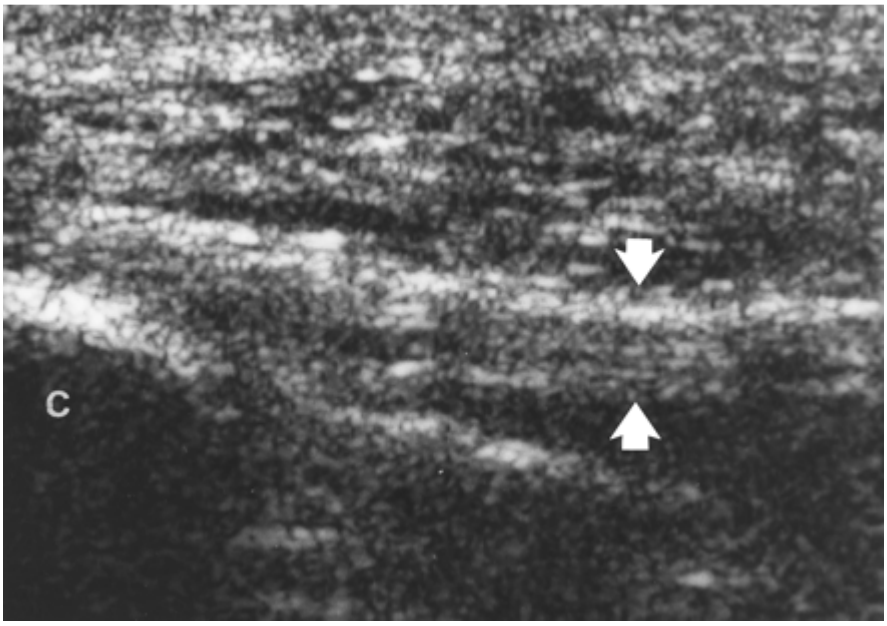

Fig. 1A. —31-year-old man with heel pain. Conventional longitudinal sonogram of plantar fascia (*arrows*) reveals normal thickness and echotexture. c = calcaneus.

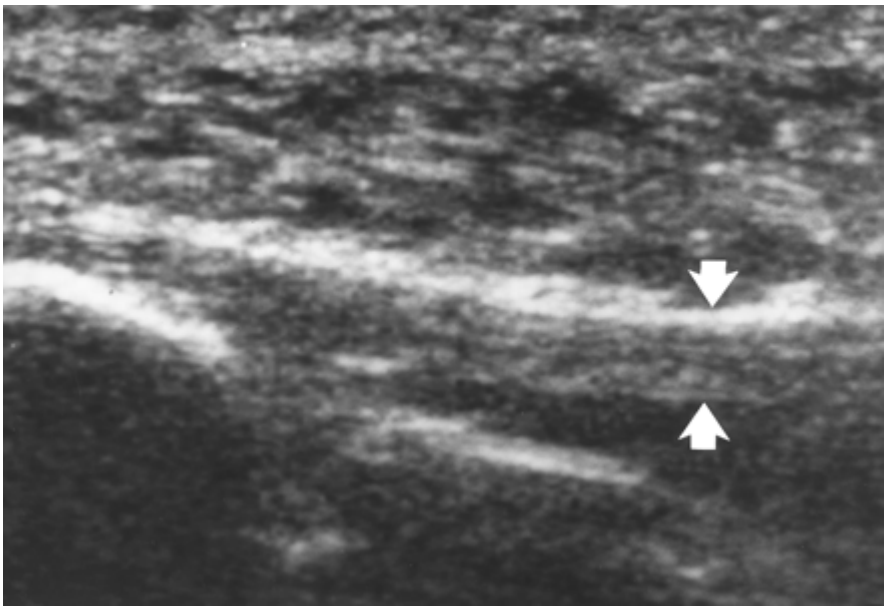

Fig. 1B. —31-year-old man with heel pain. Spatially compounded longitudinal sonogram provides better definition of both plantar fascia (*arrows*) and bony acoustic landmark of calcaneus. Note markedly reduced speckle compared with **A**, as well as decreased anisotropic effect, allowing better delineation of fibers of plantar fascia.

Further contributing to image degradation in sonography is speckle. Speckle results from interference of acoustic fields generated by the scattering of the ultrasound beam from tissue reflectors. Speckle noise is a random phenomenon and results in the characteristic grainy appearance of sonographic images [5]. By averaging images obtained from different angles of insonation, one can reduce this random phenomenon. As a result, signal-to-noise ratio is improved. As we show in this study, speckle noise is significantly reduced with compound sonography. This reduction probably also contributes to improved tissue-plane definition and image detail (Figs. 2A,2B and 3A,3B).

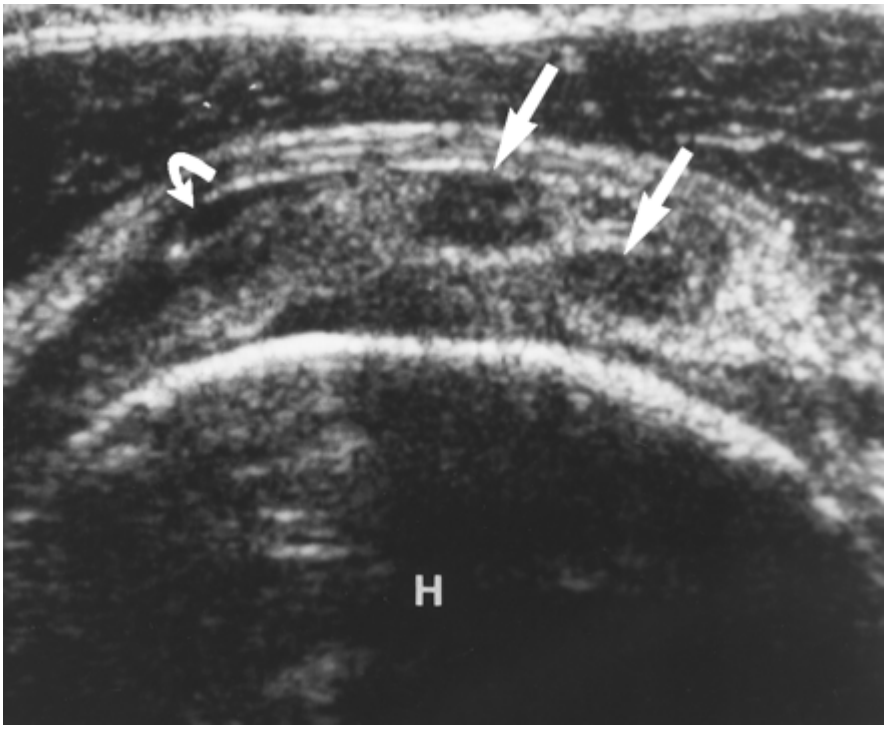

Fig. 2A. —55-year-old woman with shoulder pain. Conventional transverse sonogram of supraspinatus tendon shows complex tear (*straight arrows*) associated with small amount of fluid (*curved arrow*) in subdeltoid bursa. H = humeral head.

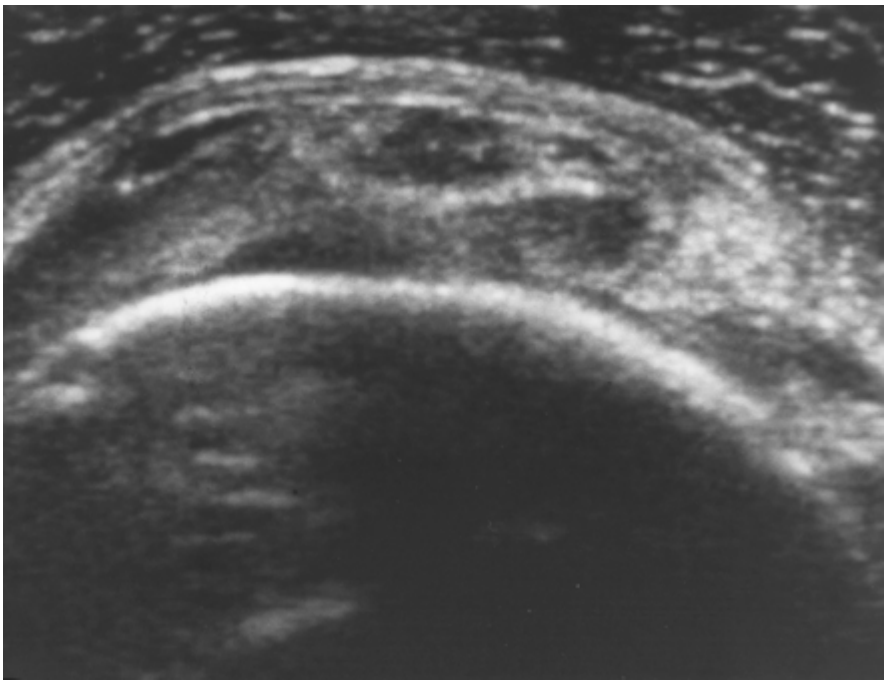

Fig. 2B. —55-year-old woman with shoulder pain. Spatially compounded transverse sonogram provides better definition of complex supraspinatus tear and of subdeltoid fluid, again because of reduced speckle.

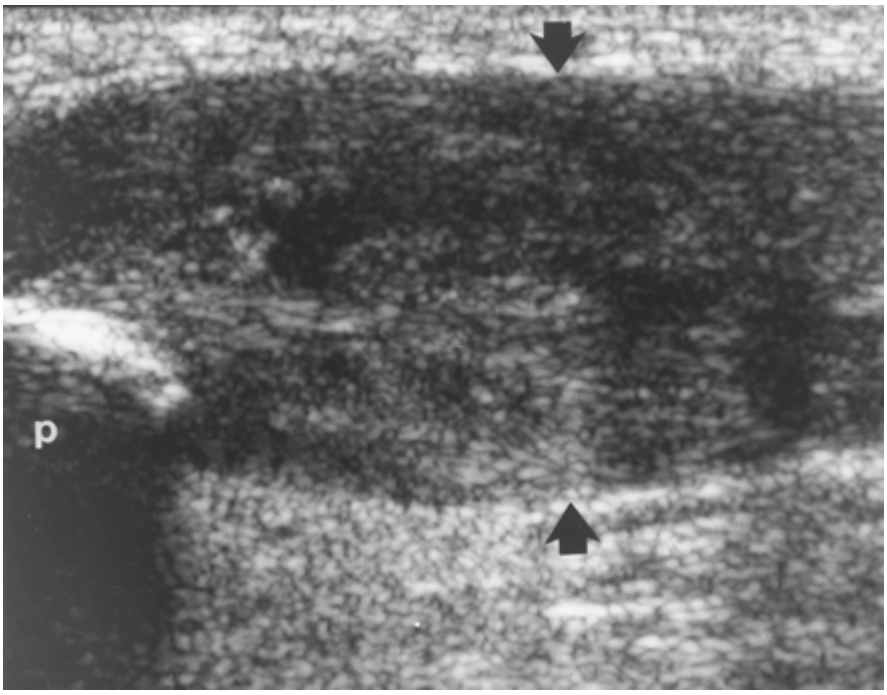

Fig. 3A. —46-year-old man with knee pain. Conventional longitudinal sonogram of proximal patellar tendon (*arrows*) just distal to patellar apex (p) shows markedly thickened and heterogeneous tendon, indicative of patellar tendonopathy.

Fig. 3B. —46-year-old man with knee pain. Longitudinal spatially compounded sonogram reveals intrasubstance tears (*straight arrows*) in patellar tendon as well as multiple tiny calcifications (*curved arrow*) not clearly seen in **A**.

One potential cost of using spatial compounding is decreased temporal resolution. Because several frames are averaged, a persistence effect results. With a greater number of frames compounded, motion blur is increasingly likely. This is potentially problematic in musculoskeletal sonography, in which a great advantage over other imaging modalities (MR imaging and CT) is the ability to image musculoskeletal structures dynamically. It has been suggested, however, that motion may not be an important problem because most musculoskeletal structures are superficial, a factor that allows high frame rates [8]. Furthermore, the number of frames averaged can be adjusted according to the application. For example, during the dynamic evaluation of tendons, a lower number of frames could be used, whereas in static situations, a higher number of frames can be compounded.

This study has several limitations. Although the reviewers of each examination were unaware of image type, the sonographers who obtained the images were not. Even for the reviewers, blinding was difficult to achieve because of the substantial differences in image quality between conventional and compound images. Although there was a qualitative improvement in image quality with compound sonography, it has not yet been shown to improve the sensitivity or specificity of musculoskeletal sonography in making particular diagnoses. The theoretic diagnostic benefits of spatial compound sonography were not evaluated in this study and remain to be shown in future research. However, preliminary data do suggest that compound sonography improves sensitivity and specificity in certain musculoskeletal settings, such as in shoulder impingement (De Candia A et al., presented at the European Congress of Radiology meeting, March 2001).

In conclusion, spatial compound sonography reduces image artifacts and thereby improves tissue-plane definition. Because musculoskeletal sonography is highly dependent on image quality and tissue-plane definition, real-time spatial compound sonography represents an important development in the field.

1. *Berson M, Roncin A, Pourcelot L. Compound scanning with an electrically steered beam. Ultrason Imaging1981;3: 303 -308*

2. *Carpenter DA, Dadd MJ, Kossoff G. A multimode real time scanner. Ultrasound Med Biol1980;6: 279 -284* CrossRefMedline
3. *Shattuck D, von Ramm OT. Compound scanning with a phased array. Ultrason Imaging1982;4: 93 -107* CrossRefMedline

4. *Jespersen SK, Wilhjelm JE, Silleson HH. Multiangle compound imaging. Ultrason Imaging1998;20: 81 -102* Medline
5. *Merritt CRB. Update in ultrasonography. Radiol Clin North Am 2001;39: 385 -397* CrossRefMedline
6. *Shapiro RS, Simpson WL, Rausch DL, Yeh HC. Compound spatial sonography of the thyroid gland: evaluation of freedom from artifacts and of nodule conspicuity. AJR2001;177: 1195 -1198* Abstract/FREE Full Text
7. *Jespersen SK, Wilhjelm JE, Silleson HH. In vitro spatial compound scanning for improved visualization of atherosclerosis. Ultrasound Med Biol 2000;26: 1357 -1362* CrossRefMedline
8. *Entrekin RR, Porter BA, Sillesen HH, et al. Real-time spatial compound imaging: application to breast, vascular, and musculoskeletal ultrasound. Semin Ultrasound CT MR2001;22: 50 -64* CrossRefMedline

Aplicações emergentes, tais como a elastografia e a US com realce de contraste foram também mencionados. A teoria da elasticidade está baseada na informação da dureza tecidual. Os módulos que avaliam as propriedades elásticas dos meios tanto isotrópicos como anisotrópicos, recorre-se freqüentemente às seguintes constantes:

- O **módulo de Young E**, que caracteriza as propriedades elásticas do meio em uma direção, determinado pela razão da tensão mecânica nesta direção e pela magnitude da deformação na mesma direção. A razão do deslocamento sob compressão e a deformação de corte segue o módulo de Young. O módulo de Young ou módulo de elasticidade. As tensões aplicadas são aproximadamente proporcionais as deformações. A constante de proporcionalidade entre elas é denominada de módulo de elasticidade ou módulo de Young. Quanto maior for este módulo, maior a tensão necessária para o mesmo grau de deformação e, portanto, mais rígido é o material. A relação linear entre essas grandezas é conhecida como lei de Hooke. Entretanto, a elasticidade linear é apenas uma aproximação, pois os materiais reais são tridimensionais e exibem algum grau de comportamento não linear. Dependendo do tipo de carga representada pelo diagrama de tensão-deformação, o módulo de elasticidade pode ser relatado como:
  - ✓ **módulo de elasticidade compressivo (ou módulo de elasticidade em compressão).** O módulo de elasticidade em tensão e compressão são aproximadamente iguais e são conhecidos como **módulo de Young**. O módulo de rigidez relaciona-se ao módulo de Young por meio da equação:

$$E = 2G(r + 1)$$

onde E é o módulo de Young (psi), G é o módulo de rigidez (psi) e r é o coeficiente de Poisson.

  - ✓ **módulo de elasticidade flexural** (ou módulo de elasticidade em flexão);
  - ✓ **módulo de elasticidade de cisalhamento** (ou módulo de elasticidade em cisalhamento). O módulo de cisalhamento quase sempre é igual ao módulo de torção e ambos são chamados de módulo de rigidez
- O **coeficiente de Poisson S,** que se define como a razão da deformação da compressão transversal pela deformação da tração longitudinal, originadas por uma tensão mecânica**.** O módulo de elasticidade também é chamado de módulo elástico e coeficiente de elasticidade. O módulo usado sozinho geralmente refere-se ao módulo de elasticidade de tração
- **O módulo de deslizamento m**, que se define como a razão do esforço de deslocamento pela deformação por cisalhamento.

A inclinação da parte em linha reta parte de um diagrama de tensão-deformação. A tangente do módulo de elasticidade é a inclinação do diagrama de tensão-deformação em qualquer ponto. A secante do módulo de elasticidade é a tensão dividida pela deformação para qualquer valor determinado de tensão ou deformação. Também é chamada de índice tensão-deformação.

Estão sendo utilizados vários tipos distintos de equipamentos médicos que impregram a elastografia:

1. Equipamentos quase estáticos
2. Equipamentos vibracionais;
3. Equipamentos que empregam ARFI ou Acoustic Radiations Fource Impulse (Sonoelastografia), que utilizam o princípio das ondas de cisalhamento

O futuro está nas sondas de silício que estão sendo investigadas para aplicação em curto prazo

.

INJEÇÕES DE PLAMA RICO EM PLAQUETAS

Apresentado por Kenneth Lee

O ultrassom é o método ideal para direcionamento da terapia com plasma rico em plaquetas (PRP). As tendinopatias acometem 7% dos pacientes, dos quais 30 a 50% decorrem de injúrias esportivas. Um tendão normal tem um aspecto histológico organizado, enquanto que na tendinopatia o padrão é desorganizado, com degeneração mucóide e necrose. O tratamento da tendinopatia inclui o alívio da dor e recuperação da função daquela estrututra, e cerca de 80% dos pacientes recuperam-se com tratamento conservador. Nos 3 a 6 meses que antecedem a resolução da tendinopatia, a dor é o sintoma mais comum. A terapia com PRP está indicada na epicondilite, na tendinopatia do manguito rotador, na tendinopatia patelar e na fásciopatia plantar. A terapia com PRP promove uma aceleração da recuperação, uma verdadeira ativação em cascata do processo regenerativo:

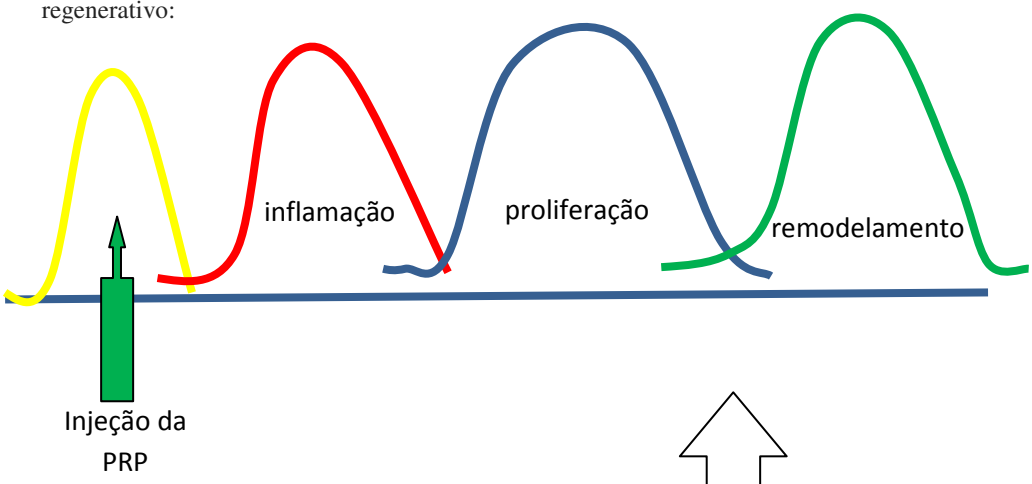

O PRP é um centrigado do sangue total:
A camada intermediária do centrifugado é extremamente rica em plaquetas e está indicado na injúria ou dor crônica de tendão/ ligamento ou sempre que houver falha no tratamento conservador.

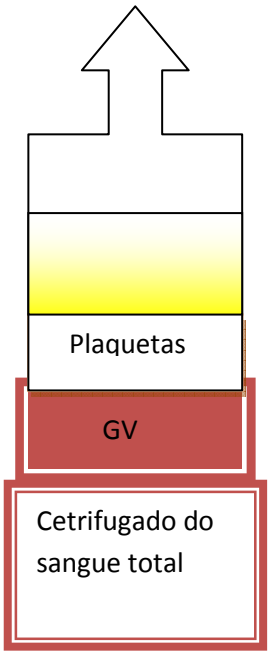

O palestrante mencionaou evidências conflitantes publicadas recentemente do valor da terapia com PRP:

1. **Am J Sports Med. 2011 Jun;39(6):1200-8. Epub 2011 Mar 21. Ongoing positive effect of platelet-rich plasma versus corticosteroid injection in lateral epicondylitis: a double-blind randomized controlled trial with 2-year follow-up.** Gosens T, Peerbooms JC, van Laar W, den Oudsten BL.

Abstract

BACKGROUND:

Platelet-rich plasma (PRP) has been shown to be a general stimulation for repair and 1-year results showed promising success percentages.

PURPOSE:

This trial was undertaken to determine the effectiveness of PRP compared with corticosteroid injections in patients with chronic lateral epicondylitis with a 2-year follow-up.

STUDY DESIGN:

Randomized controlled trial; Level of evidence, 1.

METHODS:

The trial was conducted in 2 Dutch teaching hospitals. One hundred patients with chronic lateral epicondylitis were randomly assigned to a leukocyte-enriched PRP group (n = 51) or the corticosteroid group (n = 49). Randomization and allocation to the trial group were carried out by a central computer system. Patients received either a corticosteroid injection or an autologous platelet concentrate injection through a peppering needling technique. The primary analysis included visual analog scale (VAS) pain scores and Disabilities of the Arm, Shoulder and Hand (DASH) outcome scores.

RESULTS:

The PRP group was more often successfully treated than the corticosteroid group (P < .0001). Success was defined as a reduction of 25% on VAS or DASH scores without a reintervention after 2 years. When baseline VAS and DASH scores were compared with the scores at 2-year follow-up, both groups significantly improved across time (intention-to-treat principle). However, the DASH scores of the corticosteroid group returned to baseline levels, while those of the PRP group significantly improved (as-treated principle). There were no complications related to the use of PRP.

CONCLUSION:

Treatment of patients with chronic lateral epicondylitis with PRP reduces pain and increases function significantly, exceeding the effect of corticosteroid injection even after a follow-up of 2 years. Future decisions for application of PRP for lateral epicondylitis should be confirmed by further follow-up from this trial and should take into account possible costs and harms as well as benefits.

2. **JAMA. 2010 Jan 13;303(2):144-9. Platelet-rich plasma injection for chronic Achilles tendinopathy: a randomized controlled trial**. de Vos RJ, Weir A, van Schie HT, Bierma-Zeinstra SM, Verhaar JA, Weinans H, Tol JL.

Source

Department of Orthopedics, Room Ee1614, Erasmus University Medical Center, PO Box 2040, Dr Molenwaterplein 50, 3000 CA Rotterdam, The Netherlands. r.devos@erasmusmc.nl

Abstract

CONTEXT:

Tendon disorders comprise 30% to 50% of all activity-related injuries; chronic degenerative tendon disorders (tendinopathy) occur frequently and are difficult to treat. Tendon regeneration might be improved by injecting platelet-rich plasma (PRP), an increasingly used treatment for releasing growth factors into the degenerative tendon.

OBJECTIVE:

To examine whether a PRP injection would improve outcome in chronic midportion Achilles tendinopathy.

DESIGN, SETTING, AND PATIENTS:

A stratified, block-randomized, double-blind, placebo-controlled trial at a single center (The Hague Medical Center, Leidschendam, The Netherlands) of 54 randomized patients aged 18 to 70 years with chronic tendinopathy 2 to 7 cm above the Achilles tendon insertion. The trial was conducted between August 28, 2008, and January 29, 2009, with follow-up until July 16, 2009.

INTERVENTION:

Eccentric exercises (usual care) with either a PRP injection (PRP group) or saline injection (placebo group). Randomization was stratified by activity level.

MAIN OUTCOME MEASURES:

The validated Victorian Institute of Sports Assessment-Achilles (VISA-A) questionnaire, which evaluated pain score and activity level, was completed at baseline and 6, 12, and 24 weeks. The VISA-A score ranged from 0 to 100, with higher scores corresponding with less pain and increased activity. Treatment group effects were evaluated using general linear models on the basis of intention-to-treat.

RESULTS:

After randomization into the PRP group (n = 27) or placebo group (n = 27), there was complete follow-up of all patients. The mean VISA-A score improved significantly after 24 weeks in the PRP group by 21.7 points (95% confidence interval [CI], 13.0-30.5) and in the placebo group by 20.5 points (95% CI, 11.6-29.4). The increase was not significantly different between both groups (adjusted between-group difference from baseline to 24 weeks, -0.9; 95% CI, -12.4 to 10.6). This CI did not include the predefined relevant difference of 12 points in favor of PRP treatment.

CONCLUSION:

Among patients with chronic Achilles tendinopathy who were treated with eccentric exercises, a PRP injection compared with a saline injection did not result in greater improvement in pain and activity.

2. AJR Am J Roentgenol. 2011 Mar;196(3):628-36. Musculoskeletal applications of platelet-rich plasma: fad or future? Lee KS, Wilson JJ, Rabago DP, Baer GS, Jacobson JA, Borrero CG.

Source

Department of Radiology, University of Wisconsin School of Medicine and Public Health, Madison, 53792, USA. klee2@uwhealth.org

Abstract

OBJECTIVE: The purpose of this article is to detail the biology of platelet-rich plasma (PRP), critically review the existing literature, and discuss future research applications needed to adopt PRP as a mainstay treatment method for common musculoskeletal injuries. CONCLUSION: Any promising minimally invasive therapy such as PRP deserves further investigation to avoid surgery. Diagnostic imaging outcome assessments, including ultrasound-guided needle precision, should be included in future investigations.

Ele concluiu com o protocolo para a realização do PRP:

1. A injeção única é a típica sendo rara a necessidade de injeção única;
2. Imobilização de 24 a 72 horas após o procedimento;
3. Reavaliar ;
4. Retomada gradual das atividades físicas em uma a duas semanas.